CEMCAP

Co-funded by the European Union

Grant Agreement Number:
641185

Action acronym:
CEMCAP

Action full title:
CO_2 capture from cement production

Type of action:

H2020-LCE-2014-2015/H2020-LCE-2014-1

Starting date of the action: 2015-05-01
Duration: 42 months

D11.3
Membrane-assisted CO_2 liquefaction for CO_2 capture from cement plants

Due delivery date: 2017-12-31
Actual delivery date: 2018-06-21

Organization name of lead participant for this deliverable:
SINTEF Energy Research

Project co-funded by the European Commission within Horizon2020		
Dissemination Level		
PU	Public	X
CO	Confidential , only for members of the consortium (including the Commission Services)	

Deliverable number:	D11.3
Deliverable title:	Membrane-assisted CO_2 liquefaction for CO_2 capture from cement plants
Work package:	WP11 Membrane-assisted CO_2 liquefaction
Lead participant:	SINTEF

Author(s)		
Name	**Organisation**	**E-mail**
David Berstad*	SINTEF Energy Research	david.berstad@sintef.no
Stian Trædal	SINTEF Energy Research	stian.tradal@sintef.no

*Lead author

Keywords

CO2 capture, CCS, cement, membrane, CO_2 liquefaction, process simulation, power requirement, 90 % CCR, 60 % CCR, low air leak, typical air leak

Abstract

Membrane-assisted CO_2 liquefaction is a hybrid, two-stage separation process for capturing CO_2 from flue gas. The first separation stage consists of a CO_2-selective polymeric membrane unit separating the bulk of CO_2 from the flue gas. The resulting permeate on the vacuum side of the membrane is a crude CO_2 product, still containing a considerable fraction of diluents such as nitrogen, oxygen and water. Before entering the second CO_2 separation stage, the permeate is compressed and dehydrated before it is cooled to around -54°C by recuperative and auxiliary refrigeration. In two separation stages the CO_2 is liquefied and purified for transport and storage. The gaseous separation product is recycled to the inlet of the membrane unit.

Six different cases have been evaluated. Two different cement plant flue gas compositions have been considered (with 18 mol% and 22 mol% CO_2 concentration respectively), and two main CO_2 capture ratios have been targeted (90 % and 60 %).

A multicomponent membrane model is used to simulate the membrane separation process, and this has been integrated into the interface of the commercial process simulator Aspen HYSYS. Global process models for the hybrid membrane-assisted CO_2 liquefaction process have been used in the case studies. The assumed membrane material has a selectivity of 50 for CO_2 over nitrogen, and the total membrane surface areas used in simulations are 228 000 m^3 and 152 000 m^3 for 90 % and 60 % capture ratio, respectively.

The net electric power requirement for the hybrid CO_2 capture process varies between 1066 kJ/kg_{CO2} for 60 % CO_2 capture ratio from the flue gas with 22 mol% CO_2 concentration, and 1458 kJ/kg_{CO2} for 90 % CO_2 capture ratio from the flue gas with 18 mol% CO_2 concentration. The power requirement is in all cases caused mainly by flue gas compression, vacuum pumping and compression of crude CO_2 permeate, and auxiliary refrigeration.

Compared to other end-of-pipe capture technologies, the performance of membrane-based processes is highly sensitive to CO_2 concentration in the flue gas stream. Therefore, in addition to optimising membrane materials and configurations, it is equally important to reduce the air ingress to increase CO_2 concentrations in the flue gas. This will contribute to improving the performance of membrane-assisted CO_2 liquefaction.

Please cite this report as: *Berstad, David; Trædal, Stian, 2018. Membrane-assisted CO2 liquefaction for CO2 capture from cement plants (D11.3).*

Refer to the CEMCAP community in Zenodo.org for citation with DOI.

This project has received funding from the European Union's Horizon2020 Research and Innovation Programme under Grant Agreement No 641185

TABLE OF CONTENTS

Page

This project has received funding from the European Union's Horizon2020 Research and Innovation Programme under Grant Agreement No 641185

This project has received funding from the European Union's Horizon2020 Research and Innovation Programme under Grant Agreement No 641185

1 CASE DEFINITIONS AND FLUE GAS FEED CONDITIONS

The flue gas feed stream conditions used in this work are given in Table 1 below and originate from the CEMCAP framework [1]. The dust fraction has been omitted from the composition in the simulation cases.

Table 1: Flue gas feed data for "Typical air leak" and "Low air leak".

		Typical air leak	Low air leak
Total flow rate	kg/h	388,098	318,192
Temperature	°C	110	130
CO_2	vol%	18	22
N_2	vol%	63	60
O_2	vol%	10	7
H_2O	vol%	9	11
Dust	mg/m^3_{STP}	10	10

Six different cases for CO_2 capture by membrane-assisted liquefaction have been evaluated in the present work (flue gas compositions refer to those given in Table 1):

1. 90 % CO_2 capture ratio from the "Typical air leak" flue gas composition. The required membrane area and pressure levels in the separation processes are set to give the targeted CO_2 capture ratio.
2. 90 % CO_2 capture ratio from the "Low air leak" flue gas composition, while maintaining the membrane surface area and general process configuration derived from Case no. 1. The targeted 90 % CO_2 capture ratio is obtained by adjusting flexible process parameters, primarily pressure levels.
3. 60 % CO_2 capture ratio from the "Typical air leak" flue gas composition. The required membrane area and pressure levels in the separation processes are set to give the targeted CO_2 capture ratio.
4. 60 % CO_2 capture ratio from the "Low air leak" flue gas composition. Similar as for Case no. 2, using the membrane surface area and general process configuration derived from Case no. 3, and thus obtaining the targeted 60 % CO_2 capture ratio by adjusting primarily pressure levels.
5. Maximisation of the CO_2 capture ratio when the flue gas composition in Case no. 3 changes from that of "Typical air leak" to "Low air leak". Case no. 5 uses the same membrane surface area and process configuration, including pressure levels, as for Case no. 3 to investigate the potential increase in CO_2 capture ratio.
6. An additional "what-if" case based on Case no. 1. The nitrogen permeance in the membrane is assumed to have doubled from its initial characteristics due to ageing/degradation, thus significantly reducing the CO_2 selectivity. This case investigates this effect on obtainable CO_2 capture ratio as well as energy requirement.

This project has received funding from the European Union's Horizon2020 Research and Innovation Programme under Grant Agreement No 641185

2 PROCESS UNIT DESCRIPTIONS AND SIMULATION BASIS

In the following, the process units and related assumptions used in the process simulations are described. As far as possible, it has been the aim to use the standard assumptions defined in the CEMCAP framework [1].

2.1 NOx and SOx removal

Assumptions for NOx and SOx removal units are assumed to be identical to those used in the MEA reference case modelling [2] in CEMCAP. NOx is removed by selective catalytic reduction in the cement plant while SOx is removed upstream the main blower and direct-contact flue gas cooler (see Figure 3).

The feed blower gives the flue gas a slight pressure increase, from 1.013 bar(a) to 1.05 bar(a)[1], upstream the de-SOx scrubber. The blower has an isentropic efficiency of 85 %.

2.2 Main flue gas blower

After SOx removal, the flue gas is further compressed since the polymeric membrane requires a certain pressure difference as well as pressure ratio between the feed side and permeate side. The pressure ratio across the main blower/compressor is typically in the range 2.2–2.5.

Since the volume flowrate in both blowers (de-SOx blower and main blower) are in the range of 300 000–400 000 m^3/h, these machines are assumed to be axial-fan blowers.

The first blower is likely a single-stage machine due to the low pressure ratio, while the main blower will be made up of several consecutive axial stages to obtain the required pressure ratio.

The overall isentropic efficiency of the main blower is assumed to be 85 %.

2.3 Direct-contact flue gas cooler

Before entering the membrane, the flue gas will also require cooling by direct-contact water quench. This unit is located downstream of the main flue gas blower. The opposite order would not be sensible in the membrane-assisted liquefaction application, since the compression gives the flue gas a considerable temperature increase, which would likely require another direct contact cooler stage to avoid exceeding the temperature tolerance of the membrane unit. Instead, the flue gas is compressed in a relatively warm state, and subsequently cooled.

The direct-contact cooler is modelled as a counterflow contactor column with 10 ideal stages. Hot flue gas enters in the bottom stage and flows upwards. Cooling water is fed from the top and cools the upward flowing flue gas before it is withdrawn from the bottom of the cycle. The flue gas pressure is assumed to drop by 5 kPa through the contactor.

[1] All pressures given in this document (bar, bar(a)) should be read as bar absolute. Low pressure levels as well as vacuum pressure levels are given the unit bar(a) for explicitness.

This project has received funding from the European Union's Horizon2020 Research and Innovation Programme under Grant Agreement No 641185

2.4 Polymeric membrane unit

A multicomponent membrane model developed by SINTEF Energy Research has been used to simulate the membrane separation process. See [3] for other uses of this model for other post-combustion CO_2 capture applications. The membrane model is a 1-D distributed cross flow model that makes calculations based on the following inputs:

- Feed gas mass flow, pressure and composition
- Permeate gas pressure
- Permeance of all components through membrane and membrane area, or permeance for a primary component and selectivity of all other components relative to the primary component
- Membrane surface area

Based on these inputs, the model calculates the respective chemical compositions as well as the mass flows of permeate and retentate streams.

The membrane model has been integrated into the Aspen HYSYS interface, such that it can be used flexibly on the same level as other process unit embedded in the simulation software.

The membrane data used in the simulations are listed in Table 2.

Table 2: Baseline membrane permeance data used in simulations.

Component	Permeance [m^3(STP)/m^2sPa]	Permeance [m^3(STP)/m^2bar-h]	CO_2 selectivity over other components
CO_2	$7.5 \cdot 10^{-9}$	2.7	1
N_2	$1.5 \cdot 10^{-10}$	0.054	50
O_2	$6.0 \cdot 10^{-10}$	0.216	12.5
H_2O	$1.5 \cdot 10^{-7}$	54	0.05

The feed pressure level for the membrane unit is a function of the main blower pressure ratio, as well as the pressure drop in the subsequent direct-contact cooler. Pressure drop through the membrane units is assumed to be 10 kPa.

The baseline permeate pressure level is set to 0.2 bar(a) and is obtained by using vacuum pumps on the permeate side.

2.5 Permeate vacuum pump

Although the largest mass flowrate in the membrane-assisted CO_2 capture system is found at the membrane feed side, the largest volume flowrate is found on the permeate side of the membrane. This is due to the low pressure of 0.2 bar(a). Hence, a very large vacuum pumping capacity is required, however at a moderate vacuum level. Since the membrane units will be highly modularised in a full-scale system (typically in the magnitude of hundreds or thousands of units, depending on the achievable geometry and membrane area integrated in an industrial-scale unit), it is also adequate to assume a modularised vacuum pumping system in which each vacuum pump caters to a certain number of membrane-unit bundles. A typical number of vacuum pump units for

This project has received funding from the European Union's Horizon2020 Research and Innovation Programme under Grant Agreement No 641185

the full-scale membrane-assisted liquefaction system could be 10–20, but possibly more, depending on the available machinery types and respective capacities.

In the process simulations the isentropic efficiency of each vacuum pump is assumed to be 75 %. The suction and discharge pressures are 0.2 bar(a) (baseline value) and 1.034 bar(a), respectively.

2.6 Permeate-gas cooler and retentate-gas heater

Due to the high pressure ratio, the outlet temperature from the vacuum pumps is high. In the simulation models the permeate gas is assumed to be cooled against the membrane retentate gas stream in a gas-to-gas heat exchanger. Since the retentate stream can be expanded to recover a considerable amount of power, the power recovery is enhanced by increasing the gas temperature prior to expansion. +

The minimum temperature approach in the permeate-retentate heat exchanger is set to 25 °C.

After heat exchange with the retentate gas, the permeate gas is further cooled by cooling water in a heat exchanger before the water knock-out and compression stages. The combined relative pressure drop of the permeate gas in the permeate–retentate and water-cooled heat exchangers is assumed to be 2 %. Likewise, the relative pressure drop of the retentate gas in the heat exchanger is set to 2 %.

2.7 Retentate gas expander

Since the retentate stream from the membrane unit contains a considerable amount of pressure-based energy, a significant portion of the power used for compressing the flue gas feed stream can be recovered by expanding the retentate gas before venting to the atmosphere. As mentioned in section 2.6, heating this gas prior to expansion increases both the recoverable amount of power and the outlet temperature of the vented gas.

The expander is assumed to have an overall isentropic efficiency of 85 % and an outlet pressure of 1.1 bar(a). The expander can be either a radial or axial machine with multiple expansion stages.

2.8 Permeate gas compressor train with intercooling and water knockout

After vacuum pumping, cooling and water knockout, the permeate gas enters a multi-stage compressor train with intercoolers and intermediate water knockout stages. In the simulation model, it is assumed that the permeate stream is compressed from atmospheric pressure to about 31 bar in a three-casing compressor train. Each casing, or machine, is assumed to have an overall pressure ratio of 3.20, and the machines are assumed to be centrifugal compressors. Each casing contains several centrifugal impellers to achieve this pressure ratio. The overall isentropic efficiency of each casing is assumed to be 85 %.

After each compressor, the gas is cooled to 28 °C in water-cooled heat exchangers. The free water condensing during the aftercooling is subsequently separated in water knockout drums. In two of the three aftercooling stages the hot gas is cooled partly through heat exchange with a returning "tail gas" stream from the low-temperature liquefaction process before it is further cooled to 28 °C

This project has received funding from the European Union's Horizon2020 Research and Innovation Programme under Grant Agreement No 641185

by cooling water. For these two stages, the inter-/aftercooling process is therefore divided into two heat exchanger stages, where the high-quality portion of the heat is utilised for heating the cold, returning tail gas stream. The relative pressure drop for each intercooling stage including water knockout is assumed to be 2 %.

2.9 Molsieve desiccant bed for dehydration

After the last water knockout stage, the permeate gas stream still contains a saturated fraction of water vapour. Due to the low temperatures and elevated pressure levels in the low-temperature CO_2 liquefaction unit, deeper dehydration is mandatory for preventing water ice formation in the colder heat exchangers. Dehydration by solid desiccants such as molsieve adsorbent beds is state of the art in most cryogenic applications such as air separation and natural gas liquefaction.

By using measurement data for water vapour pressure over ice [4], the maximum allowable water concentration can be calculated for different temperature and pressure levels. Figure 1 shows the maximum water concentration for the pressure interval 20–34 bar for the -45, -50 and -55 °C isotherms. As can be observed, the water concentration must be reduced to < 1 ppm when temperature levels of -55 °C are to be applied. Such deep level of dehydration requires the use of solid desiccant beds.

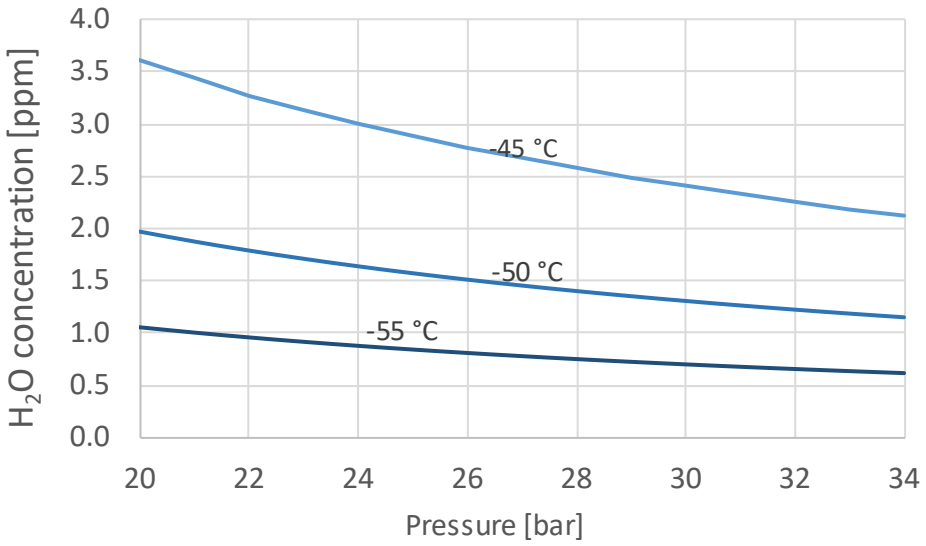

Figure 1. Maximum water concentration to avoid ice formation for different temperature and pressure levels.

The dehydration unit is assumed to consist of at least two solid desiccant beds. At least on bed is in active mode adsorbing water at any time to ensure continuous operation of the CO_2 liquefaction process. Once the bed has been saturated with water, the gas is diverted to another parallel unit. The operation of the previously active bed is interrupted, and the bed is switched from active mode to regeneration mode. Regeneration is primarily done by temperature swing, where a gas, for instance a small stream of dry, captured CO_2, is heated to 200–300 °C and is used to desorb the water from the solid bed. Once the regeneration operation is completed the bed has been re-activated and is available for dehydration.

This project has received funding from the European Union's Horizon2020 Research and Innovation Programme under Grant Agreement No 641185

In the simulations, the bed is represented as a continuous process unit removing practically all water from the moist and compressed permeate stream. Pressure drop through the molsieve bed is assumed to be 0.5 bar.

2.10 Coldbox heat exchanger network

After dehydration the CO_2-rich, dry permeate stream is cooled in a series of four low-temperature heat exchangers. Two of the heat exchangers are internal "process-to-process" recuperators and in the two others, the gas is cooled by auxiliary refrigeration. Each of the four heat exchangers are assumed to have an absolute pressure drop of 0.4 bar. The minimum temperature approach in these heat exchangers is set to 3 °C.

2.11 Auxiliary refrigeration

Auxiliary refrigeration is assumed to be supplied by standard industrial, single-component vapour-compression cycles. The high-temperature stage (-42 °C evaporation temperature) is assumed to be a two-stage propane cycle in cascade with a single-stage ethane low-temperature stage (-57 °C evaporation temperature).

2.12 Separation vessels

There are two separation vessels in the CO_2 liquefaction process. The first separation is assumed to take place at -54 °C and about 29 bar, and this stage separates the main portion of CO_2 in liquid form. The second separation takes place at about -55 °C and 8.5 bar. The main purpose of the second separation is to increase the purity of captured CO_2 from 95.5 % to > 99 %. If sufficient residence time is allowed, the composition and flowrate of the separation liquid and vapour separation products are expected to be close to equilibrium conditions.

The expected CO_2 liquid yield and thus separation ratio for each separator can be estimated using equilibrium data for CO_2 mixtures. If Y_0, Y and X denote respectively the CO_2 mol fraction in the feed stream, vapour product stream and liquid product stream of the separator, the estimated CO_2 separation ratio can be expressed as:

$$CCR = \frac{X(Y_0 - Y)}{Y_0(X - Y)} \quad (1)$$

Phase equilibrium compositions estimated for the binary CO_2/N_2 system is plotted in Figure 2 for up to 50 bar separation pressure and separator temperatures between -55 °C and -35 °C. In all simulated cases, equilibrium conditions are assumed to be obtained in the separation vessels.

The purified liquid CO_2 product is pumped to a higher pressure and reheated before pumped to the final state at 110 bar pressure. The gas-phase separation product from the first separator is the "tail gas" from the liquefaction process, and this is recycled back to the membrane unit. The gas-phase separation product from the second separator is recycled internally in the CO_2 liquefaction process.

This project has received funding from the European Union's Horizon2020 Research and Innovation Programme under Grant Agreement No 641185

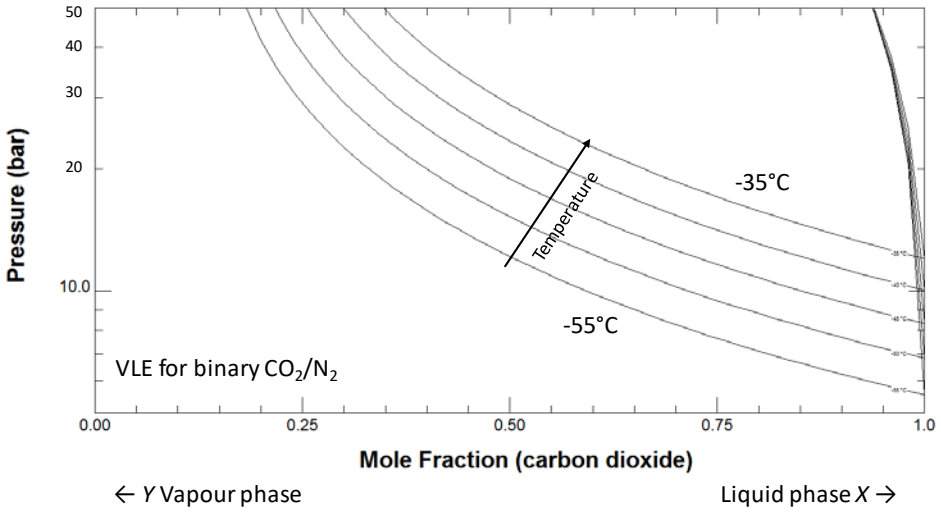

Figure 2. Vapour-liquid equilibrium data for the binary CO_2/N_2 system. Data generated from [5].

2.13 CO_2 pumping and reheating

The liquid CO_2 product is pumped to delivery pressure (110 bar) in two stages. The first pumping stage raises the pressure of the cold liquid CO_2 to 60 bar. Pressurisation by liquid pumping requires a very low amount of power input since the liquid CO_2 is incompressible and has high density. After pumping to 60 bar the CO_2 is reheated to about ambient temperature against the permeate feed stream in a recuperative counterflow heat exchanger. After reheating, the CO_2 is still in liquid form and has very low compressibility. The final delivery pressure is obtained by a second liquid CO_2 pumping stage.

The actual volume flow of liquid CO_2 is extremely low compared to the equal CO_2 flowrate in gaseous form, which makes the compression equipment compact. In the simulations, the liquid CO_2 pumps have an isentropic efficiency of 80 %. The relative pressure drop of the liquid CO_2 stream in the heat exchanger is assumed to be 2 %.

2.14 Internal recycle compressor

A certain amount of CO_2-rich flash gas is generated in the throttling at the inlet of the second separator. To avoid otherwise reduced CO_2 capture ratio, this flash gas stream is recycled to the inlet of the low-temperature heat exchanger network, where it is mixed with the main permeate feed stream prior to cooling.

A recycle compressor is required to compress the flash gas stream to match the pressure of the permeate feed. This compressor is small in volume flow and power requirement compared to the compressors in the permeate feed compressor train. The compressor is assumed to be a multi-stage centrifugal machine without inter- or aftercoolers, with an overall isentropic efficiency of 85 %.

Another feasible option for recompressing the stream would be to recycle it to a matching stage pressure-wise in the permeate compressor train. The advantage would be a reduction in the number of compressors, while there are some obvious potential disadvantages. Mixing of a cold stream

This project has received funding from the European Union's Horizon2020 Research and Innovation Programme under Grant Agreement No 641185

with a hot, moist stream could cause issues regarding water ice formation at the point of mixing. The mixing of temperatures would also lead to thermodynamic losses, in turn potentially increasing the power penalty of the process.

2.15 Tail gas reheating, expansion and recycling

The tail gas from the first separator contains a fraction of non-liquefied CO_2. At the given separation pressure and temperature (see section 2.12), this stream is still expected to have a higher CO_2 concentration than that of the flue gas from the cement plant. Hence, this stream can be recycled to the inlet of the polymeric membrane to enable a higher CO_2 capture ratio than would otherwise be obtained if this stream were to be purged directly. Due to the resulting increase in feed flowrate for the membrane unit, the membrane surface area requirement will increase to a certain extent.

Since the pressure level of the tail gas stream is significantly higher than that of the membrane feed, a considerable amount of energy recovery is possible by expanding the stream in power recovery expanders. The stream is also, as for the liquid CO_2, used to precool the permeate feed stream in a counterflow recuperative heat exchanger. After heating to almost ambient temperature, the stream is further heated against waste heat from the compressor train (see section 2.8) to maximise the recoverable power output from expansion.

The tail gas stream is heated by compressor waste heat and expanded in power recovery expanders in two consecutive stages. Minimum internal temperature approach in the waste heat exchangers is set to 25 °C and the relative pressure drop on the tail-gas side is set to 2 %. Both power recovery expanders are assumed to be radial machines with an overall isentropic efficiency of 85 %.

The outlet pressure of the second expander is set to match the membrane unit inlet pressure.

2.16 Electric drive efficiency and generator power efficiency

In the current energy calculations for the membrane-assisted CO_2 liquefaction process, all power inputs and outputs are converted to an electric-power equivalent through the following efficiencies:

- 95 % electric drive efficiency for compressors
- 95 % electric generator efficiency for power recovery expanders

A certain reduction of power requirement and investment costs may be achievable by enabling direct drive for certain compressors by aligning compressors and expanders on the same shaft. This, however, requires detailed design and solutions for the given compression and expansion units, which has not been further considered in this work. The direct coupling of compressors and expanders has further implications on the physical location of the process units in consideration, as well as on the process controllability and flexibility. These are important issues to be addressed before a final process design can be made.

By assuming full conversion between electric and mechanical power, it is assumed that all compressors and expanders can be operated more independently, since there are no requirements for power balance between certain units.

This project has received funding from the European Union's Horizon2020 Research and Innovation Programme under Grant Agreement No 641185

2.17 Other assumptions

All cases have been simulated in steady-state and equilibrium mode in Aspen HYSYS, using the Peng-Robinson cubical equation of state.

This project has received funding from the European Union's Horizon2020 Research and Innovation Programme under Grant Agreement No 641185

3 90 % CO_2 CAPTURE CASES

3.1 Design case: Process description and simulation – medium air leak, 90 % CO_2 capture

The principal process flow diagram of the membrane-assisted CO_2 liquefaction process is shown in Figure 3. After front-end cooling SOx removal, the flue gas is compressed to 2.55 bar(a) by the main blower. Since the temperature is 153 °C after compression, the flue gas is cooled by direct-contact water cooling to 36 °C. Before entering the membrane units, the flue gas is mixed with a recycle stream from the CO_2 liquefaction unit, which enriches the CO_2 concentration from 19.29 mol% to 20.17 mol%. The volume flowrate of the aggregate stream increases by 18 %.

With the membrane properties given in Table 2 and feed- and permeate-side pressure levels of 2.55 and 0.2 bar(a), respectively, the total membrane area to achieve 90 % CO_2 capture ratio is estimated to 228 000 m^2.

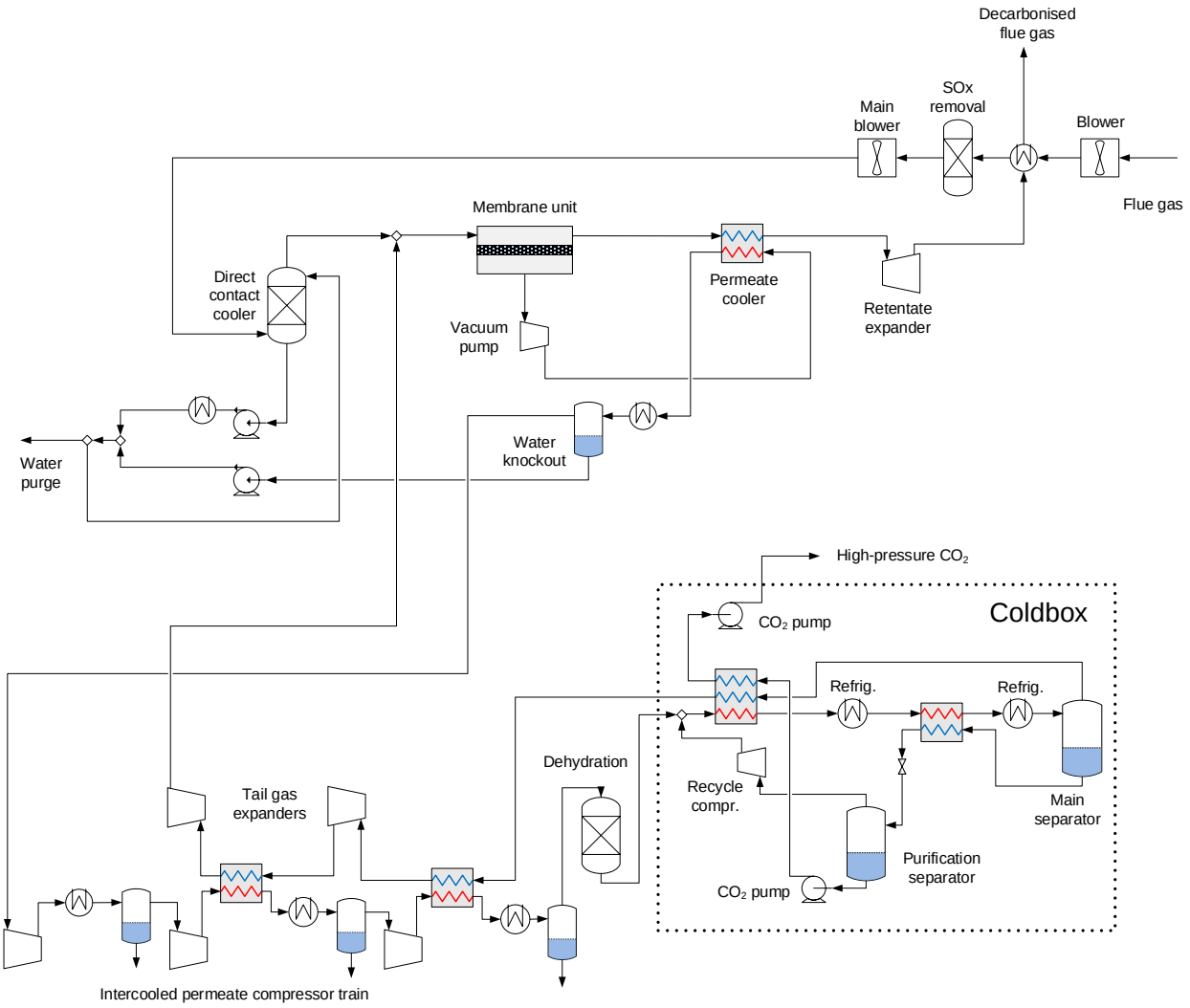

Figure 3. Process flow diagram for the membrane-assisted CO_2 liquefaction process.

This project has received funding from the European Union's Horizon2020 Research and Innovation Programme under Grant Agreement No 641185

The membrane enriches the CO_2 concentration from a feed concentration of 20.17 mol% to a permeate concentration of 56.66 %. At the vacuum pump outlet, the pressure is 1.034 bar(a) and the temperature about 220 °C. Part of this generated waste heat is utilised by heating the retentate stream to about 120 °C in a gas-to-gas heat exchanger, before the retentate stream is expanded to near-atmospheric pressure in a power recovery turbine. After the heat exchange, the permeate stream is cooled to 28 °C against cooling water in an additional heat exchanger. All condensed water is separated in a water knockout drum before the permeate stream enters the three-stage intercooled permeate gas compressor train.

After the final compression stage, the pressure is approximately 31 bar and the residual water fraction is removed in a molsieve desiccant bed. The dry permeate stream with a CO_2 concentration of 60.3 mol% is thereafter fed to the coldbox and cooled to -54 °C in a heat exchanger network made up of internal heat recuperators as well as auxiliary refrigeration heat exchangers. At -54 °C the gas mixture is partially condensed, and a CO_2-rich liquid phase is separated from the CO_2-depleted gaseous phase, or tail gas, in a knockout drum. The latter stream has a CO_2 concentration of 24.8 mol%, which is higher than that of the flue gas feed stream, and it contains almost 22 % of the CO_2 in the permeate stream. Hence, to enhance the overall CO_2 capture ratio, the tail gas stream is recycled back to the membrane inlet and mixed with the pressurised flue gas. To improve the power recovery and thus energy efficiency in the process, the tail gas is heated and expanded to a pressure level equal to that of the membrane feed in two expander stages.

The CO_2-rich liquid phase separated from the knockout drum has a purity of 95.35 mol%, provided sufficient retention time to approach equilibrium composition. To further increase the purity the stream is heated to about -42 °C and throttled to 8.5 bar and -55 °C, and further separated in a secondary knockout drum. The flash gas occurring in the throttling process contains 8 % of the CO_2 from the throttled stream and has a CO_2 concentration of 65.37 mol%. This flash gas stream is recompressed in a recycle compressor and recycled to the coldbox feed stream.

The purified liquid CO_2 stream from the second separator has a purity of 99.36 mol%, provided sufficient retention time to approach equilibrium composition. To pressurise this stream from 8.5 bar to 110 bar delivery pressure, the liquid is pumped in two stages. First the stream is pumped to 60 bar before being heated to 6.5 °C in a three-stream internal recuperator. At the outlet, the liquid CO_2 is still subcooled and can thus be further pumped to 110 bar in a second pumping stage.

Absolute and specific power results for the typical air leak case with 90 % CO_2 capture ratio are shown in Figure 4 and Figure 5, respectively. The power demand is clearly dominated by the duties of the main blower ("Blower 2") and vacuum pumps, as well as permeate compressors and auxiliary refrigeration. A considerable amount of power can be recovered from turbines to reduce the net power requirement. As can also be observed, the pressurisation of liquid CO_2 is negligible due to the low power requirements involved.

For 95 % electric-to-mechanical efficiency, the resulting net specific electric power requirement is calculated to 1458 kJ/kg_{CO2}.

This project has received funding from the European Union's Horizon2020 Research and Innovation Programme under Grant Agreement No 641185

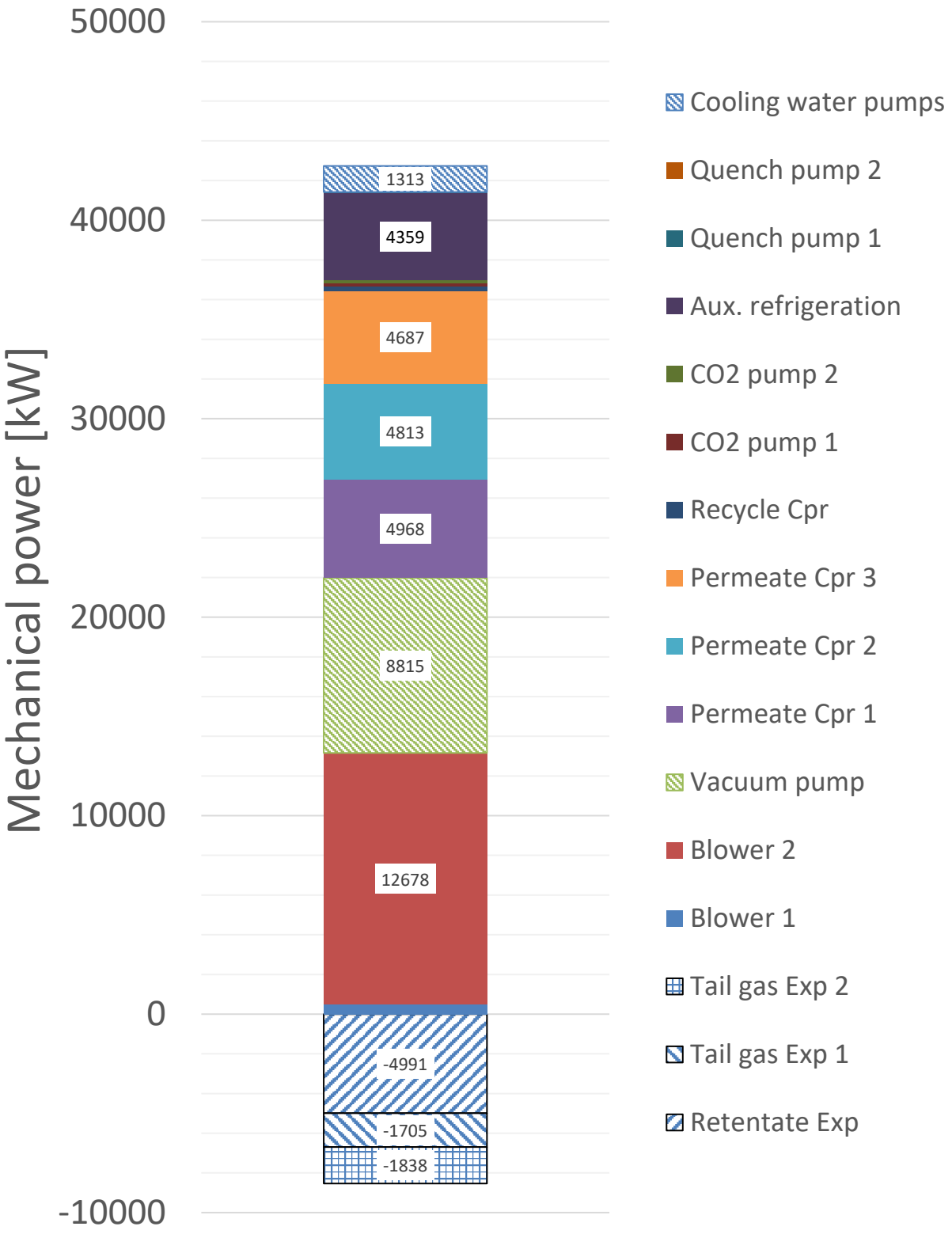

Figure 4. Decomposed results for power input and output for Case no. 1.

This project has received funding from the European Union's Horizon2020 Research and Innovation Programme under Grant Agreement No 641185

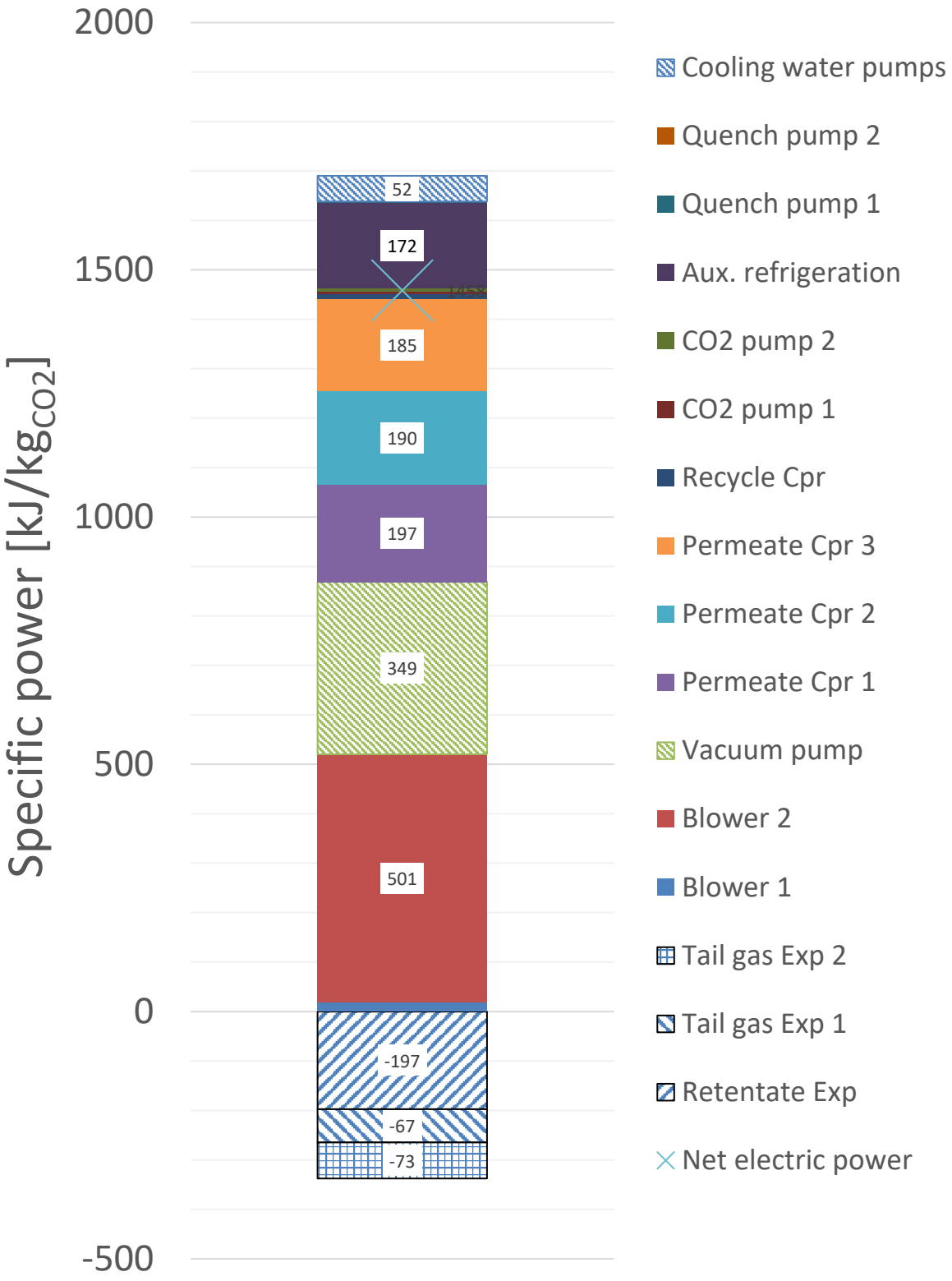

Figure 5. Decomposed specific power input and output results for Case no. 1.

This project has received funding from the European Union's Horizon2020 Research and Innovation Programme under Grant Agreement No 641185

3.2 Off-design case: Process description and simulation – Low air leak, 90 % CO_2 capture

The process modelling and simulations for the "Low air leak" conditions are performed using the same process design and membrane area as for the "Typical air leak" base case, but in an otherwise off-design configuration. The purpose is to see how the operational parameters, e.g. pressure levels, should be changed and configured relative to the base case to obtain around 90 % CO_2 capture ratio when the flue gas conditions change to higher CO_2 concentration and lower volume flowrate. The "Low air leak" flue gas conditions are more favourable than those of the "Typical air leak" base case with respect to CO_2 capture using polymeric membranes, and the specific energy requirement should thus decrease.

The process simulations are aimed at optimising the process performance for a rigorous output specification of 90 % CO_2 capture ratio, by altering the processing conditions through the existing process control options. Process control options are first and foremost those involving modified pressure levels, e.g. the membrane feed pressure delivered by the main flue gas blower, the vacuum-side pressure delivered by the vacuum pumps, and the first-stage permeate separation pressure delivered by the permeate compressor train. In the following simulations it is assumed that moderate pressure alterations and changes in volume flowrates can be achieved without affecting the respective compressor efficiencies.

Since the flue-gas CO_2 concentration increases from 18 to 22 mol%, the pressure ratio across the membrane can be lowered to obtain comparable CO_2 flux. The membrane feed and vacuum pressure levels are set to 2.23 bar(a) and 0.23 bar(a), respectively. This decreases the power requirement of the main blower as well as the vacuum pumps. Despite the reduced pressure ratio across the membrane, the resulting CO_2 enrichment of the permeate is still improved from the typical air leak case, from 56.66 mol% to 60.49 mol%. Pressure levels and temperature levels in the low-temperature part of the process are kept unchanged. Due to the increased permeate CO_2 concentration, the internal liquid yield of the low-temperature CO_2 separation process is increased from 78 % to 82 %.

The various improvements in efficiency result in a reduced power requirement compared to the typical air leak case. Gross power requirement is reduced from 42.7 MW (typical air leak) to 35.3 MW (low air leak). The main reduction in gross power requirement is caused by significant reduction in the main blower (-3.7 MW), vacuum pumps (-1.8 MW) and permeate compression (-1.6 MW). The net specific electric power requirement is calculated to 1253 kJ/kg_{CO2}, that is, a 13.7 % reduction from the typical air leak case.

The comparison of results emphasises the sensitivity to flue gas feed CO_2 concentration for the power requirement of the membrane-assisted CO_2 liquefaction process.

This project has received funding from the European Union's Horizon2020 Research and Innovation Programme under Grant Agreement No 641185

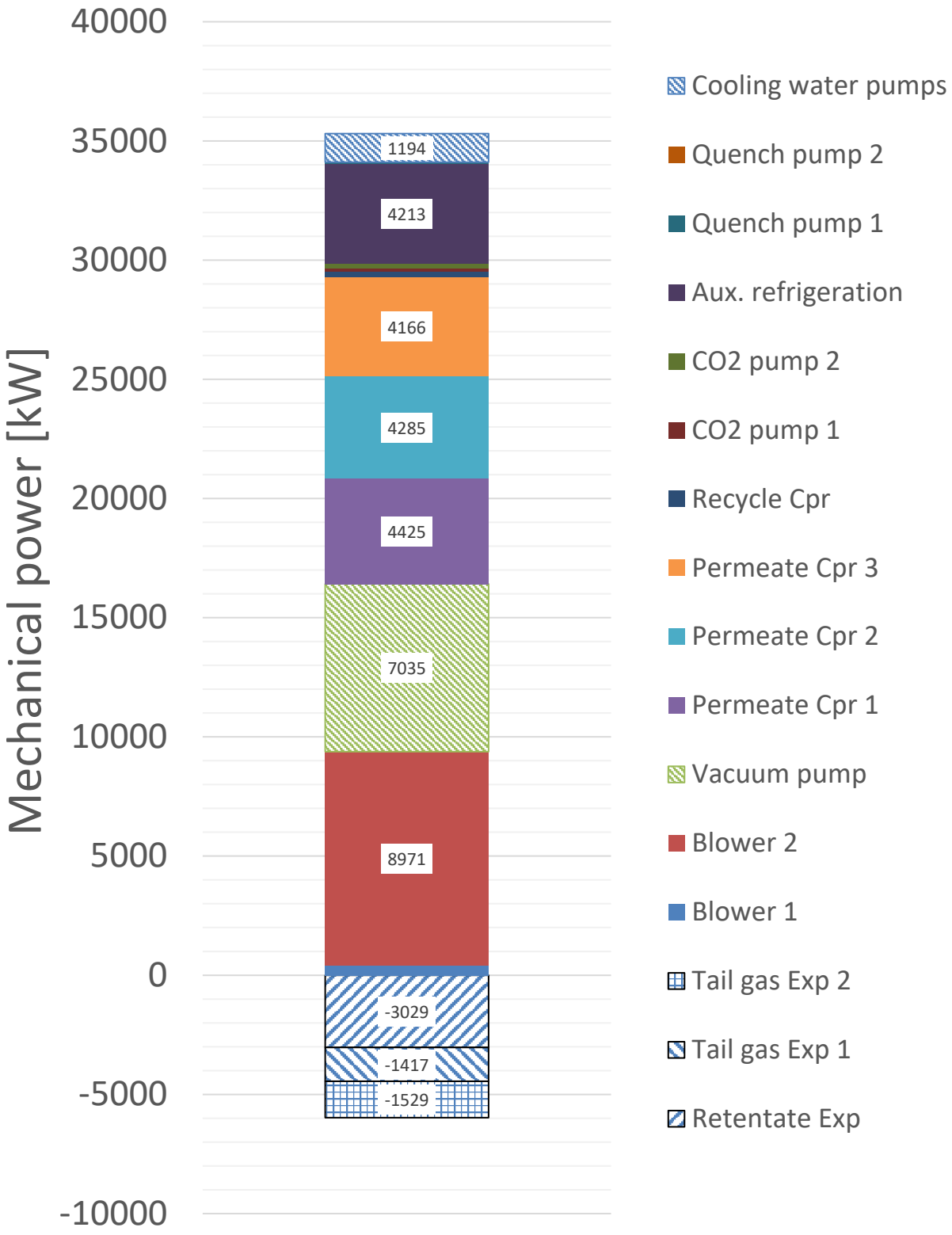

Figure 6. Decomposed results for power input and output for Case no. 2.

This project has received funding from the European Union's Horizon2020 Research and Innovation Programme under Grant Agreement No 641185

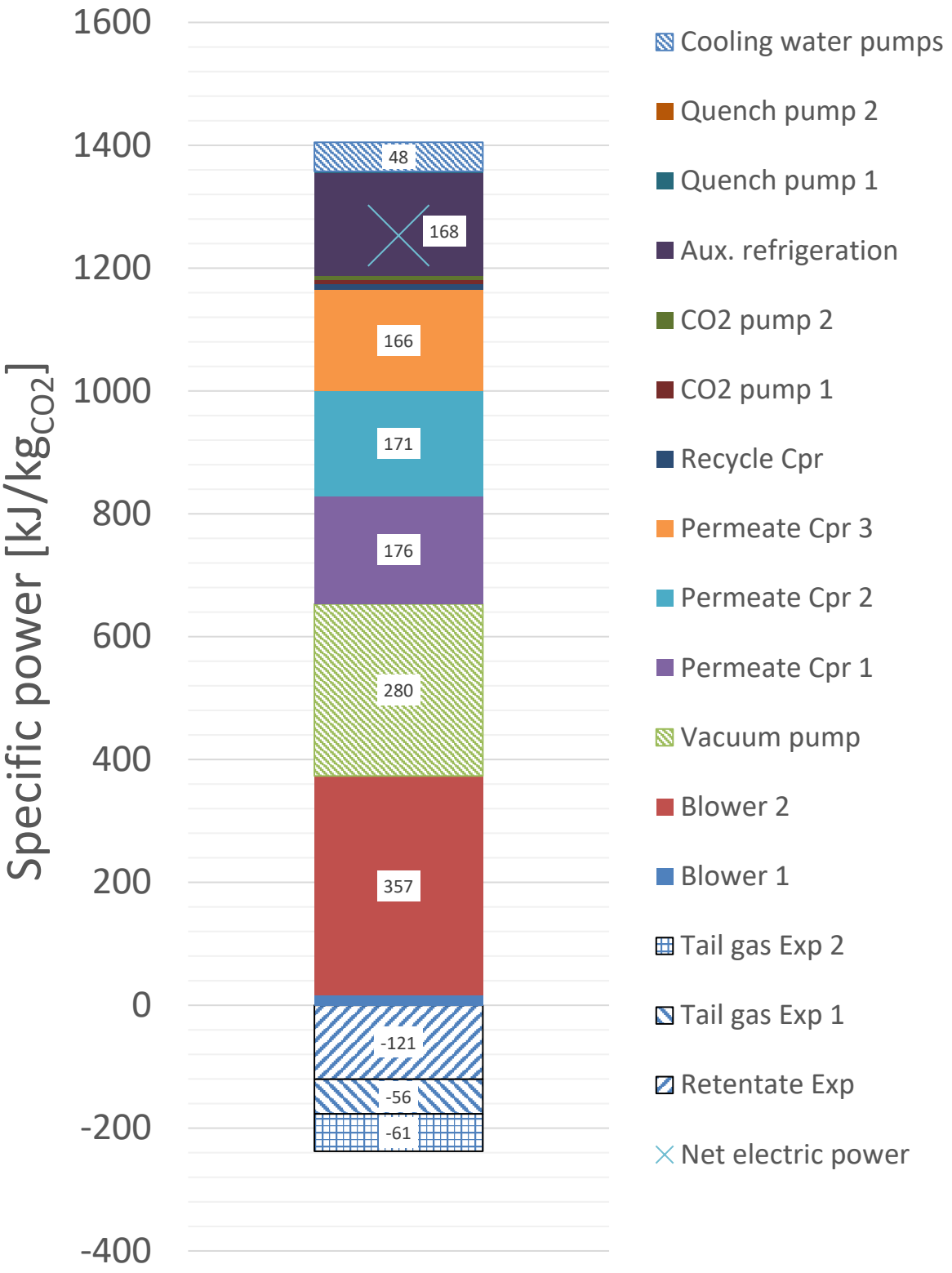

Figure 7. Decomposed specific power input and output results for Case no. 2.

This project has received funding from the European Union's Horizon2020 Research and Innovation Programme under Grant Agreement No 641185

4 PARTIAL CAPTURE CASES – 60 % CO_2 CAPTURE RATIO

4.1 Design case: Process description and simulation – typical air leak, 60 % CO_2 capture

For the partial capture cases the process design is assumed to be identical to the principal schematic shown in Figure 3. The main difference between the process setups is a significantly lower membrane surface area, combined with a lower degree of pressurisation of the flue gas. While lower membrane surface area can reduce the investment cost, the effect of lower flue gas pressurisation can contribute to significant reductions in specific power requirement for CO_2 capture and compression, as well as reduced investment cost through fewer blower stages.

Whereas the flue gas is compressed to 2.55 bar(a) in the 90 % capture case with typical air leak, the corresponding pressure level is 1.6 bar(a) in the current case. This reduces the main blower power requirement by about 47 %, from 12.7 MW to 5.9 MW. The total membrane surface area is set to 152 000 m^2, reduced by one-third, from 228 000 m^2 in the typical air leak case with 90 % capture.

The vacuum-side pressure of the membrane is set to 0.2 bar(a), and the vacuum pump discharge pressure is unchanged from the other cases. Although the pressure ratio across the membrane is lower in the current case than in the 90 % capture case, the CO_2 concentration of the permeate is still higher, 59.6 mol% and 71.1 mol% before and after knockout and drying, versus 56.7 mol% and 60.3 mol%. This leads to a generally higher liquid yield in the low-temperature CO_2 liquefaction process, about 87 % in the 60 % capture case versus 78 % in the 90 % capture case.

For the permeate compression and subsequent dehydration, the pressure levels have been kept unchanged from the 90 % capture case. This also applies to the process configuration of the CO_2 separation and liquefaction process inside the coldbox. Hence, Figure 3 represents the process flow diagram of the 60 % capture case.

Energy results are summarised in Figure 8 (absolute number, kW) and Figure 9 (specific numbers, kJ/kg captured CO_2). The main blower and vacuum pumps are, as for the 90 % capture case, the major drivers of power requirement. The resulting net specific electric power requirement is calculated to 1246 kJ/kg_{CO2}, which is about 15 % lower than for the typical air leak case with 90 % CO_2 capture.

This project has received funding from the European Union's Horizon2020 Research and Innovation Programme under Grant Agreement No 641185

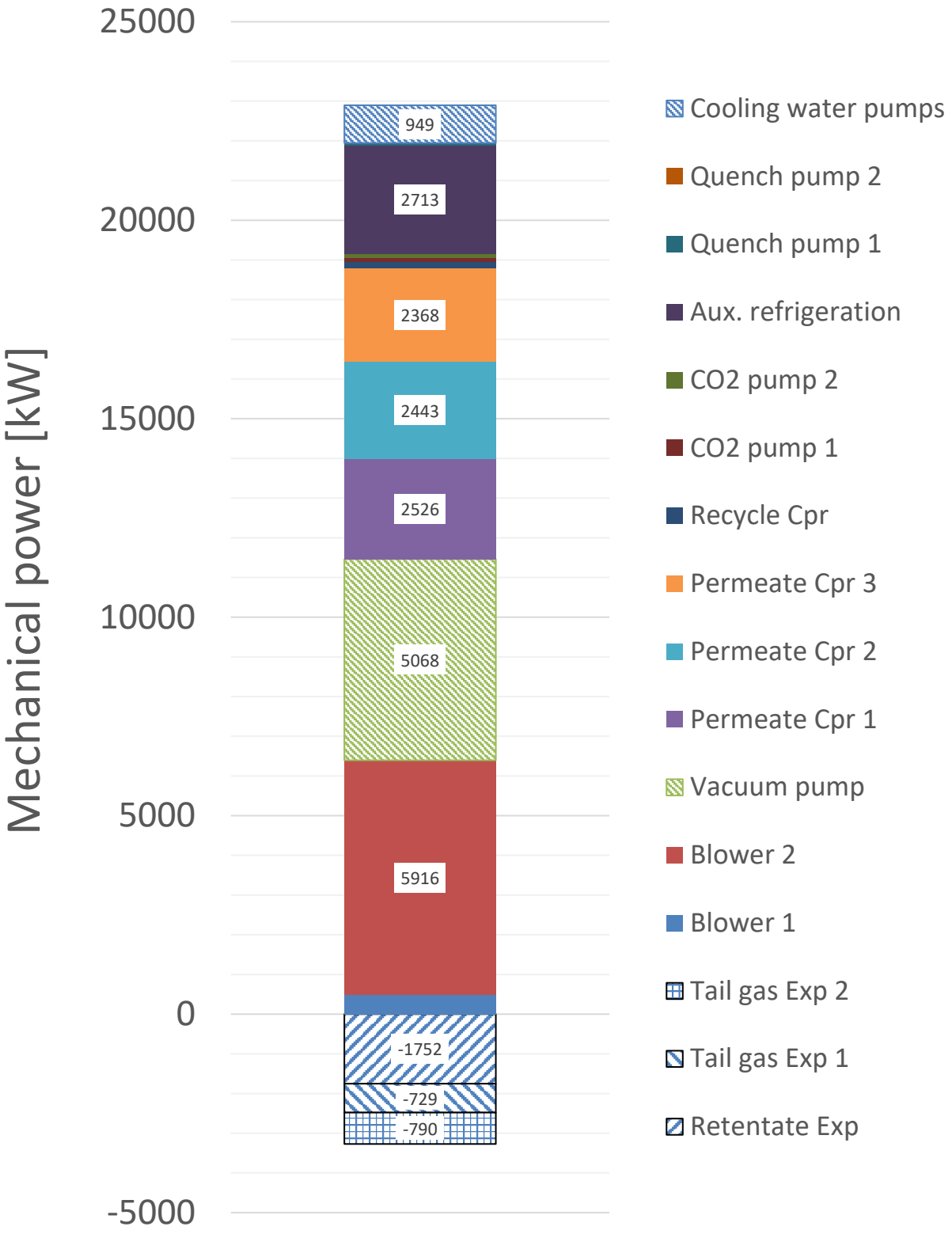

Figure 8. Decomposed results for power input and output for Case no. 3.

This project has received funding from the European Union's Horizon2020 Research and Innovation Programme under Grant Agreement No 641185

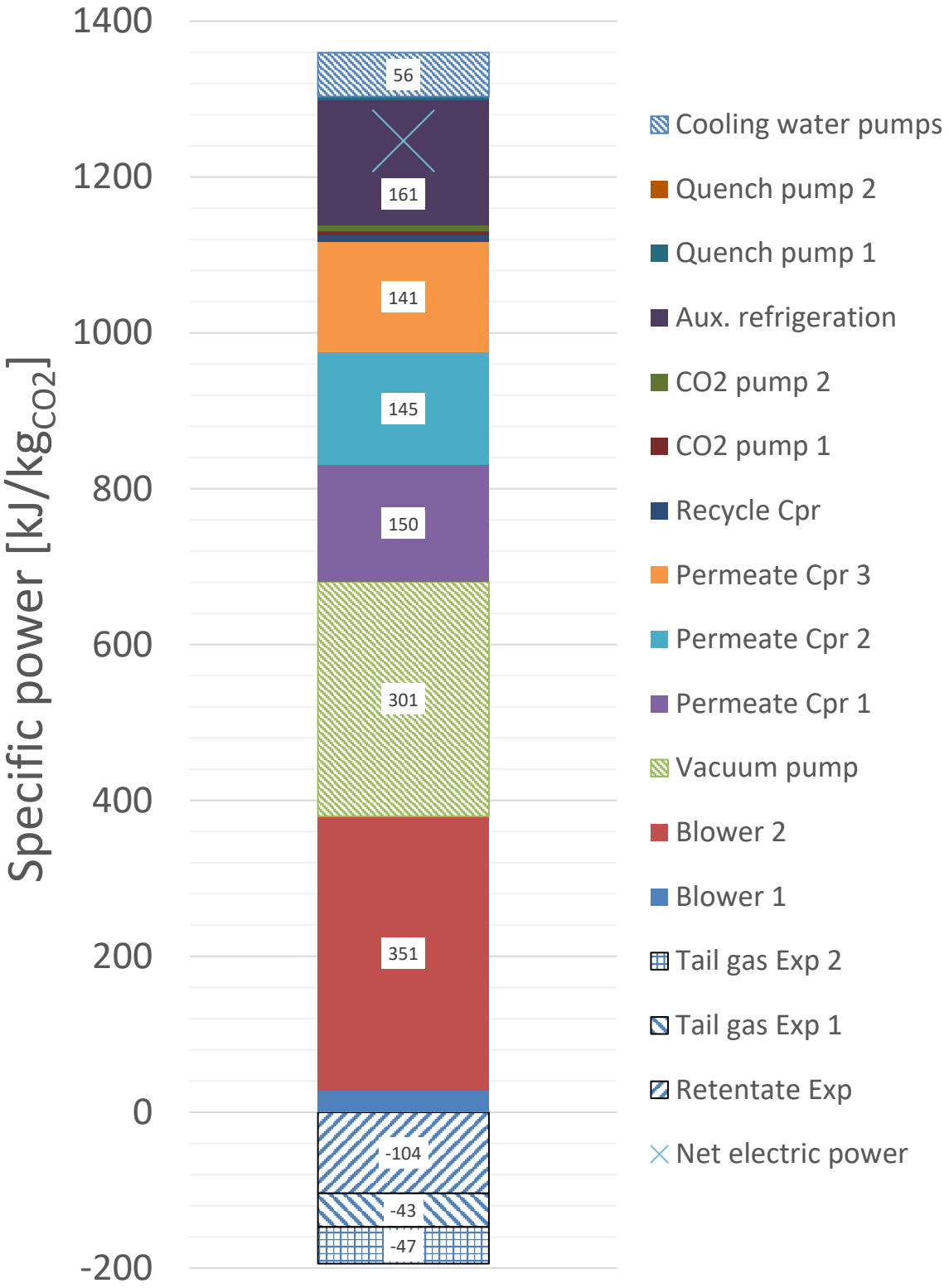

Figure 9. Decomposed specific power input and output results for Case no. 3.

This project has received funding from the European Union's Horizon2020 Research and Innovation Programme under Grant Agreement No 641185

4.2 Off-design case: Process description and simulation – low air leak, 60 % CO_2 capture

The capture process modelling and simulations for the "Low air leak" conditions with 60 % CO_2 capture ratio are based on the same process design and membrane area as for the "Typical air leak" case with 60 % CO_2 capture ratio. As for the 90 % cases, some pressure levels are modified to increase the overall energy efficiency for the same output CO_2 capture ratio. This applies to the main-blower discharge pressure, which is lowered from 1.6 bar(a) to 1.33 bar(a), while the permeate pressure is kept unchanged at 0.2 bar(a).

For this configuration, the permeate CO_2 concentration is 63.3 mol%, and increases to 76.4 mol% after water knockout and dehydration. The internal CO_2 liquid yield of the low-temperature separation and condensation unit is 90 %.

The resulting CO_2 capture ratio is estimated to 60.5 %, and the energy results are summarised in Figure 10 and Figure 11. The net specific electric power requirement is estimated to 1066 kJ/kg_{CO2}, which is 14.4 % lower than for the typical air leak case with 60 % CO_2 capture. The reduction is mainly due to lower power requirement for flue gas compression, which is reduced by 52 %, from 5.9 MW to 2.8 MW, in addition to general reductions also in vacuum pumping and permeate compression.

This project has received funding from the European Union's Horizon2020 Research and Innovation Programme under Grant Agreement No 641185

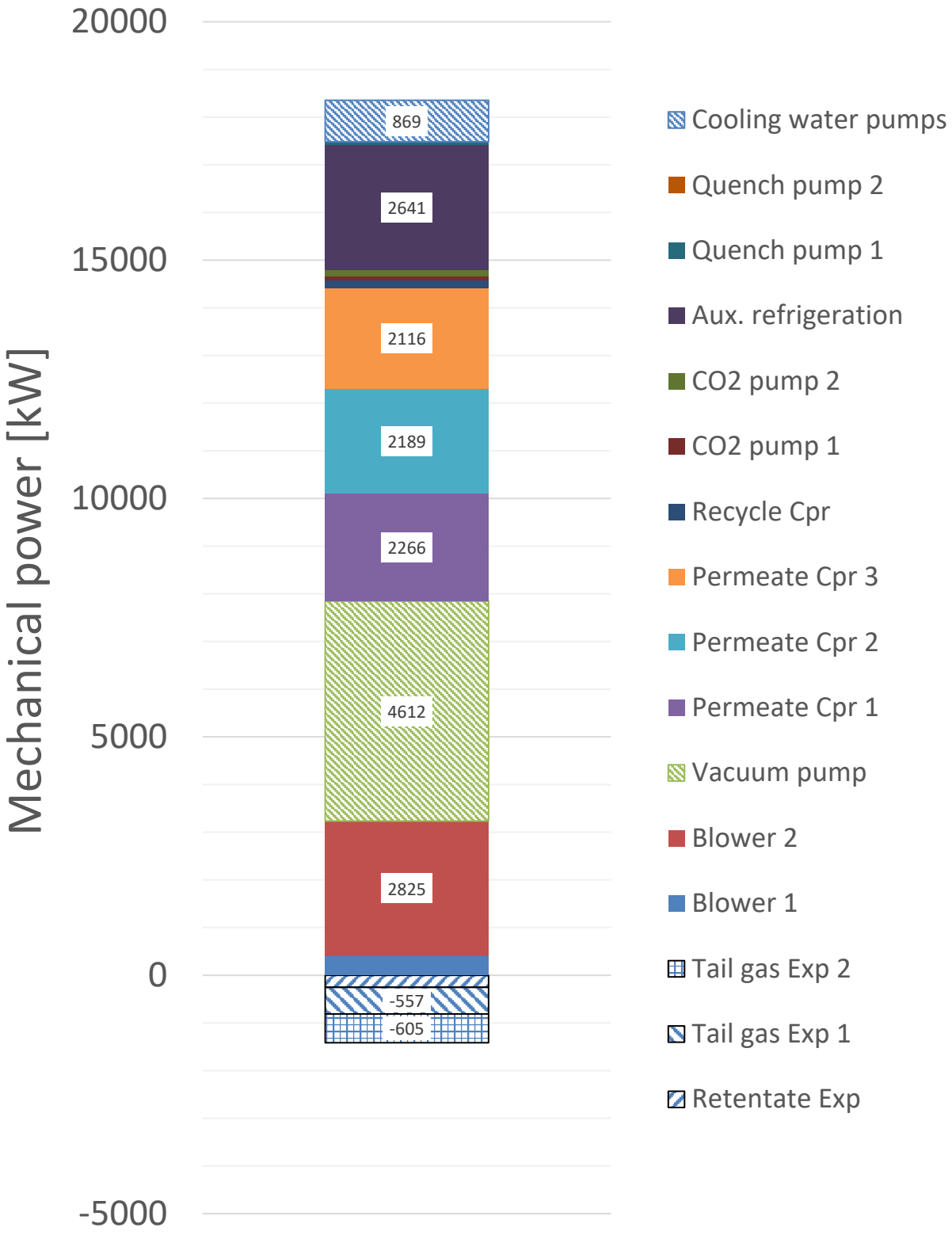

Figure 10. Decomposed results for power input and output for Case no. 4.

This project has received funding from the European Union's Horizon2020 Research and Innovation Programme under Grant Agreement No 641185

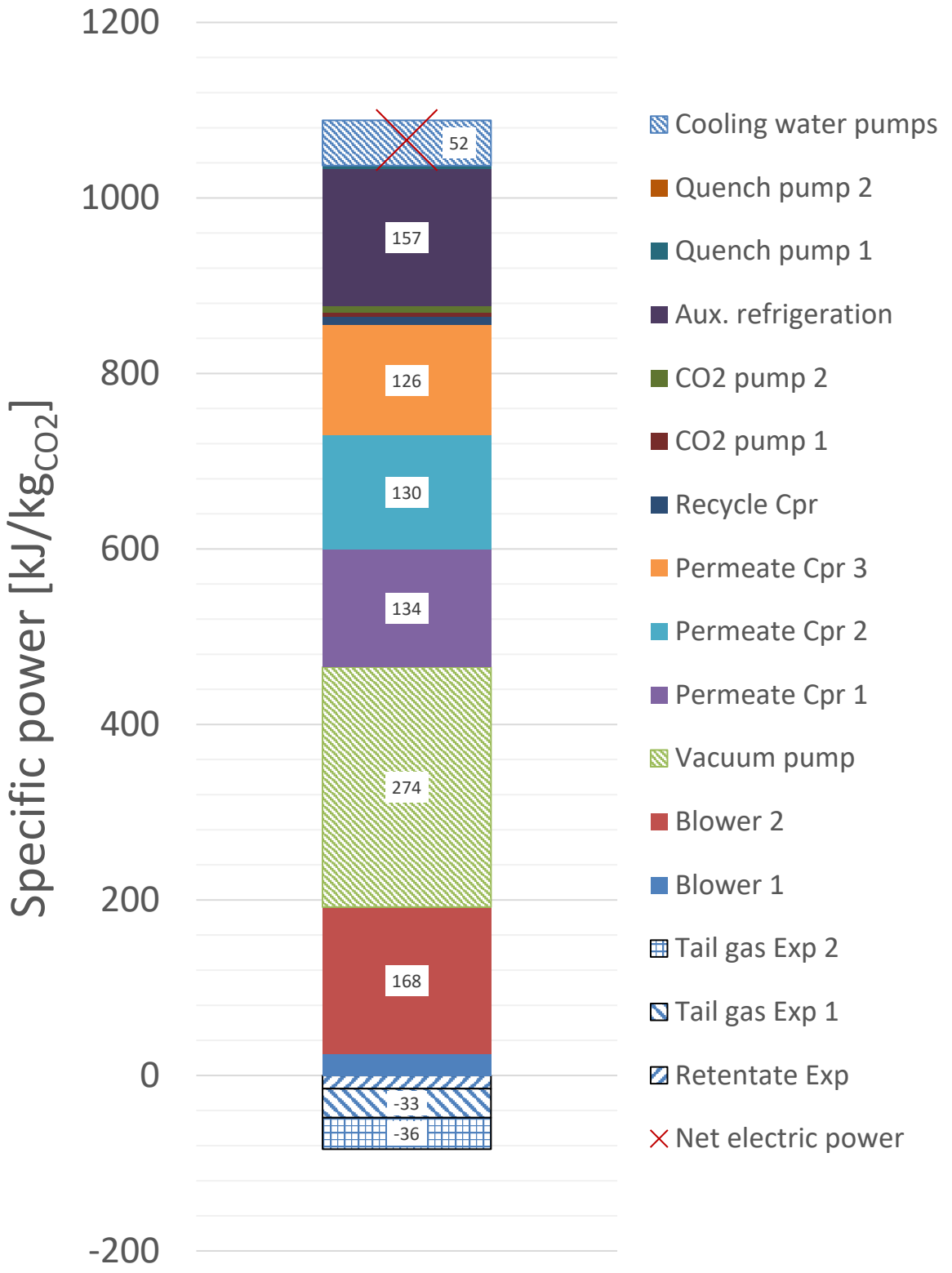

Figure 11. Decomposed specific power input and output results for Case no. 4.

This project has received funding from the European Union's Horizon2020 Research and Innovation Programme under Grant Agreement No 641185

4.3 Off-design case: Process description and simulation – low air leak, 71 % CO_2 capture

In this off-design case, all pressure levels are unchanged from the "Typical air leak" case with 60 % CO_2 capture ratio. Hence, no particular CO_2 capture ratio is targeted, and this is thus a dependent result variable rather than a targeted parameter. When the feed and vacuum-side pressure levels are unchanged, the permeate CO_2 concentration is estimated to 64.5 mol%, and 75.1 mol% after water knockout and dehydration. This concentration results in 89 % internal CO_2 liquid yield in the low-temperature separation and condensation unit.

The resulting CO_2 capture ratio is estimated to 70.9 %, with a net specific electric power requirement of 1098 kJ/kg_{CO2}, which is 3 % higher than the 60 % CO_2 capture ratio off-design case with reduced membrane feed pressure. Energy results are summarised in Figure 12 and Figure 13.

This project has received funding from the European Union's Horizon2020 Research and Innovation Programme under Grant Agreement No 641185

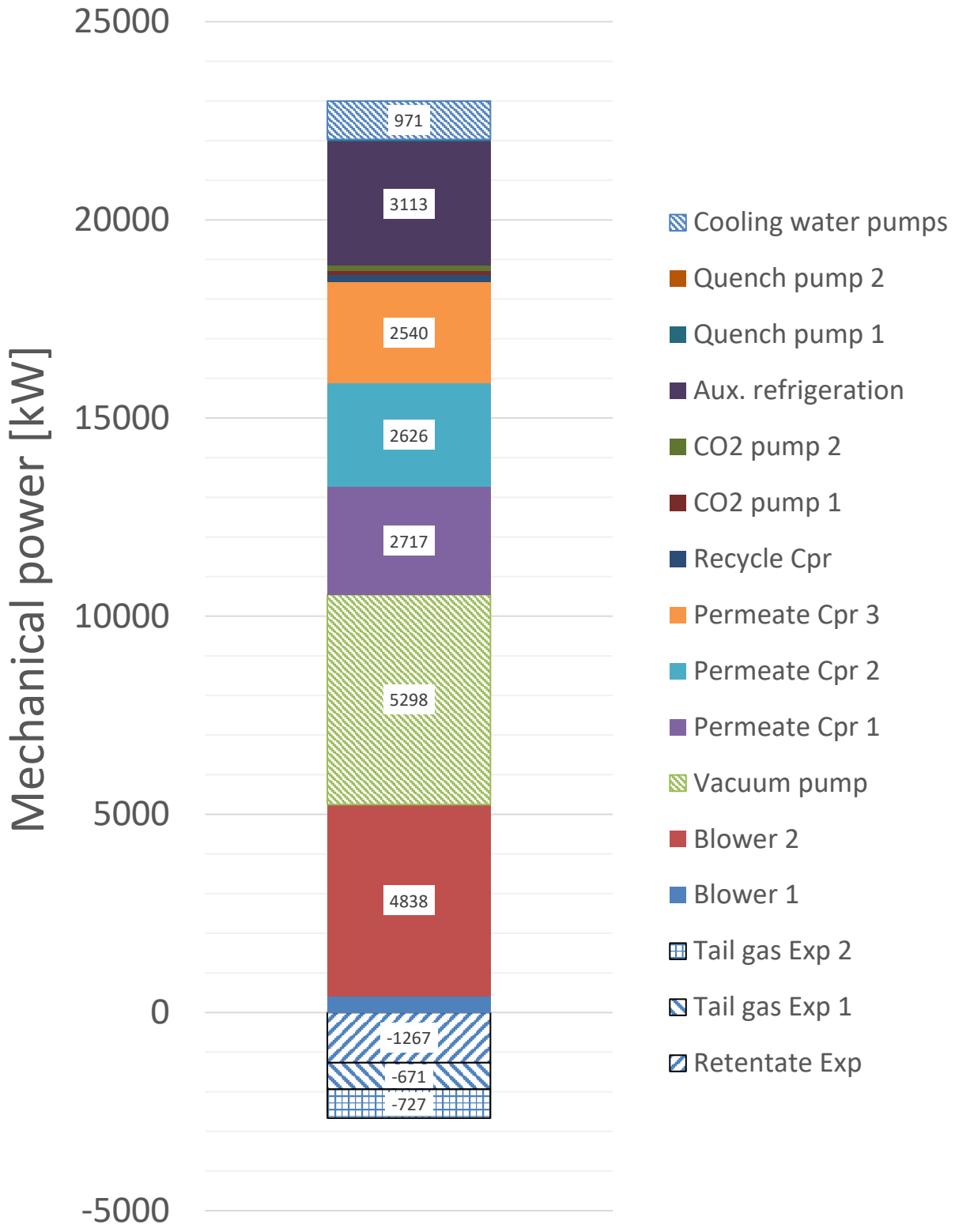

Figure 12. Decomposed results for power input and output for Case no. 5.

This project has received funding from the European Union's Horizon2020 Research and Innovation Programme under Grant Agreement No 641185

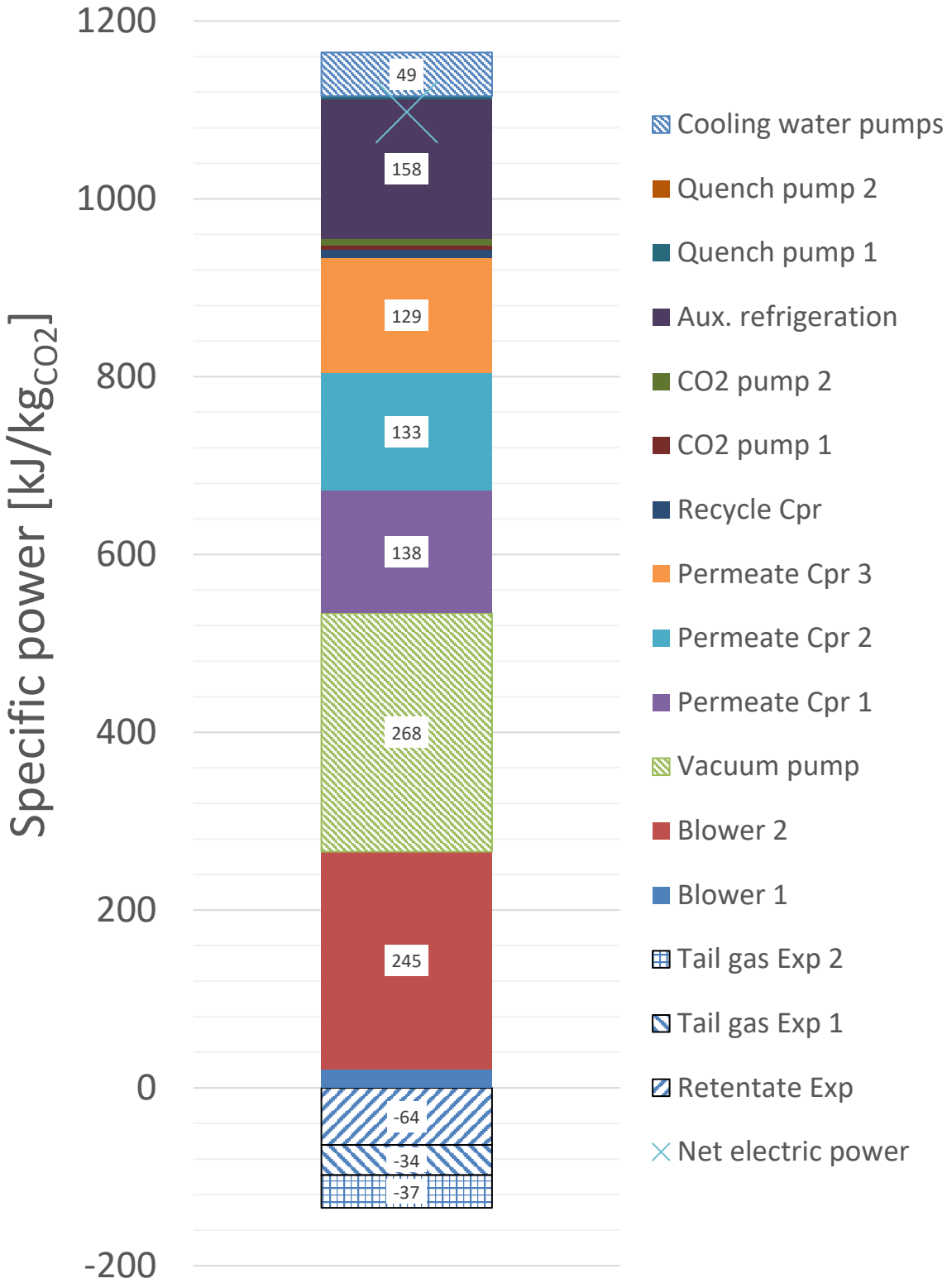

Figure 13. Decomposed specific power input and output results for Case no. 5.

This project has received funding from the European Union's Horizon2020 Research and Innovation Programme under Grant Agreement No 641185

5 MEMBRANE DEGRADATION CASE – REDUCED CO_2 SELECTIVITY

Membrane ageing and degradation of its characteristics relative to initial conditions can have different effects on the overall process performance. An additional "what-if" simulation case has been performed, for which the membrane is assumed to have changed from its initial characteristics due to ageing/degradation. The main purpose of the following simulation case is to check the principal effects on the overall capture process performance.

The degradation is assumed to be represented by a doubling of the nitrogen permeance given in Table 2, and thus reduced CO_2/N_2 selectivity.

5.1 Typical air leak case with reduced CO_2/N_2 selectivity and CCR: Process description and simulation

The simulation case for degraded membrane performance is derived from the typical air leak, 90 % CO_2 capture case described in section 3.1.

For a 100 % increase in nitrogen permeance, the main change observed in the process model is an increased flowrate through the membrane. The permeate stream becomes more diluted due to the increased nitrogen flux. This applies if the pressure difference across the membrane is unchanged from that of the baseline case, in which the feed and permeate pressures are 2.5 bar(a) and 0.2 bar(a), respectively. Unchanged pressure levels are however not possible to maintain unless the vacuum pumps have considerably redundant capacity. In the present degradation case, this is assumed not to be the case and consequently, operational parameters must be altered to give the same volume flowrate on the permeate side.

The baseline value for vacuum-side volume flowrate is about 594 000 m^3/h. In order to retain a constant vacuum pump flowrate at 0.2 bar(a) vacuum level, two process changes are assumed to be made:

- Partial purge of the flue gas feed: 13.5 % of the flue gas feed is bypassed the membrane unit and directly purged through the stack
- Reduction of membrane feed pressure: pressure is reduced from 2.5 bar(a) to 2 bar(a)

Power results for the degradation case, as well as direct comparison with the baseline case, are given in Figure 14 and Figure 15. As can be observed in Figure 14, the blower power requirement is reduced considerably due to the combination of purge and lowered discharge pressure, while the vacuum pump power requirement is practically unchanged due to equal volume flowrate and suction pressure level. However, as is observed in Figure 15, the specific power requirement still increases from 1458 to 1541 kJ/kg_{CO2} due to the considerable drop in CO_2 capture ratio, from 90 % to 71 %.

This project has received funding from the European Union's Horizon2020 Research and Innovation Programme under Grant Agreement No 641185

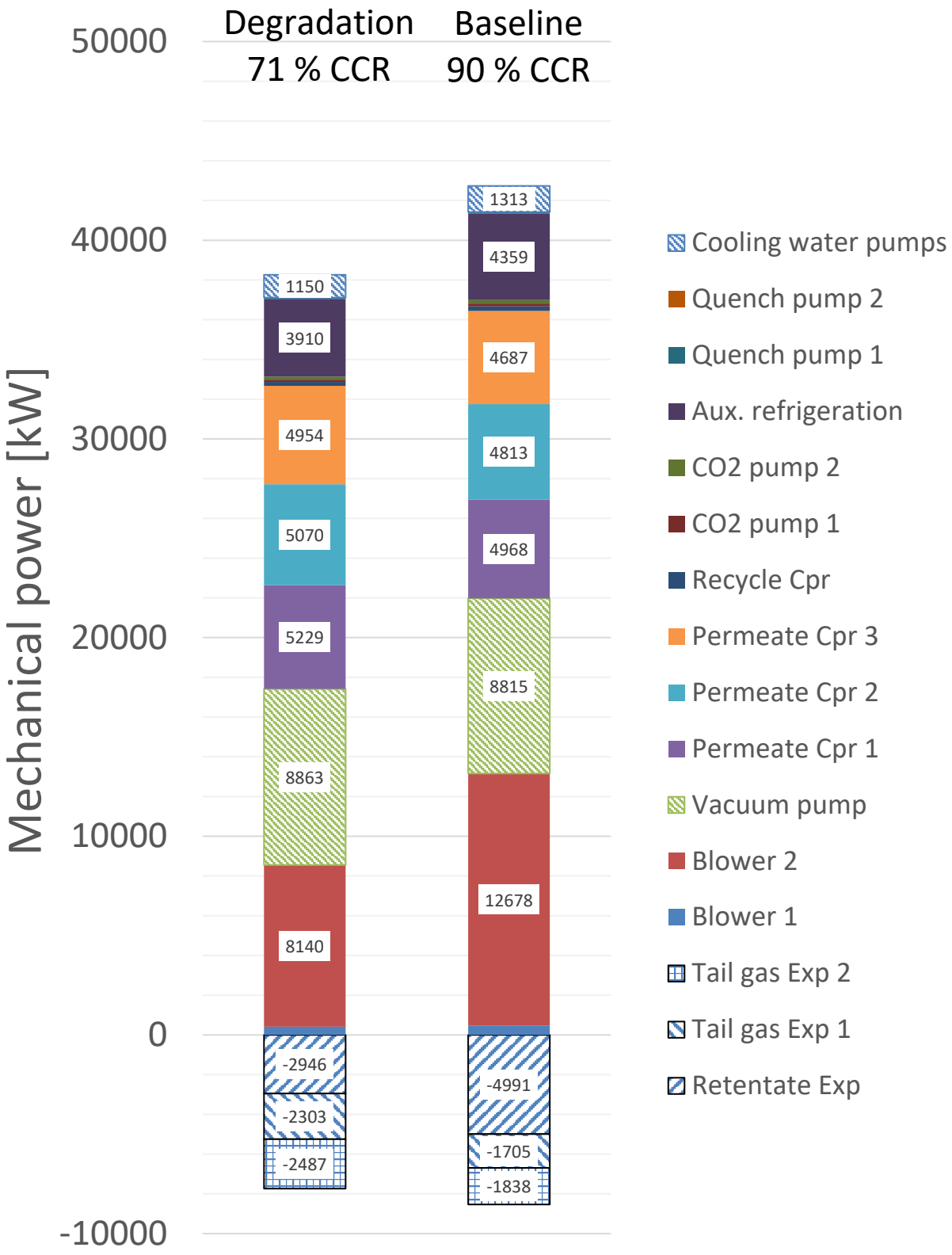

Figure 14. Decomposed results for power input and output for Case no. 6.

This project has received funding from the European Union's Horizon2020 Research and Innovation Programme under Grant Agreement No 641185

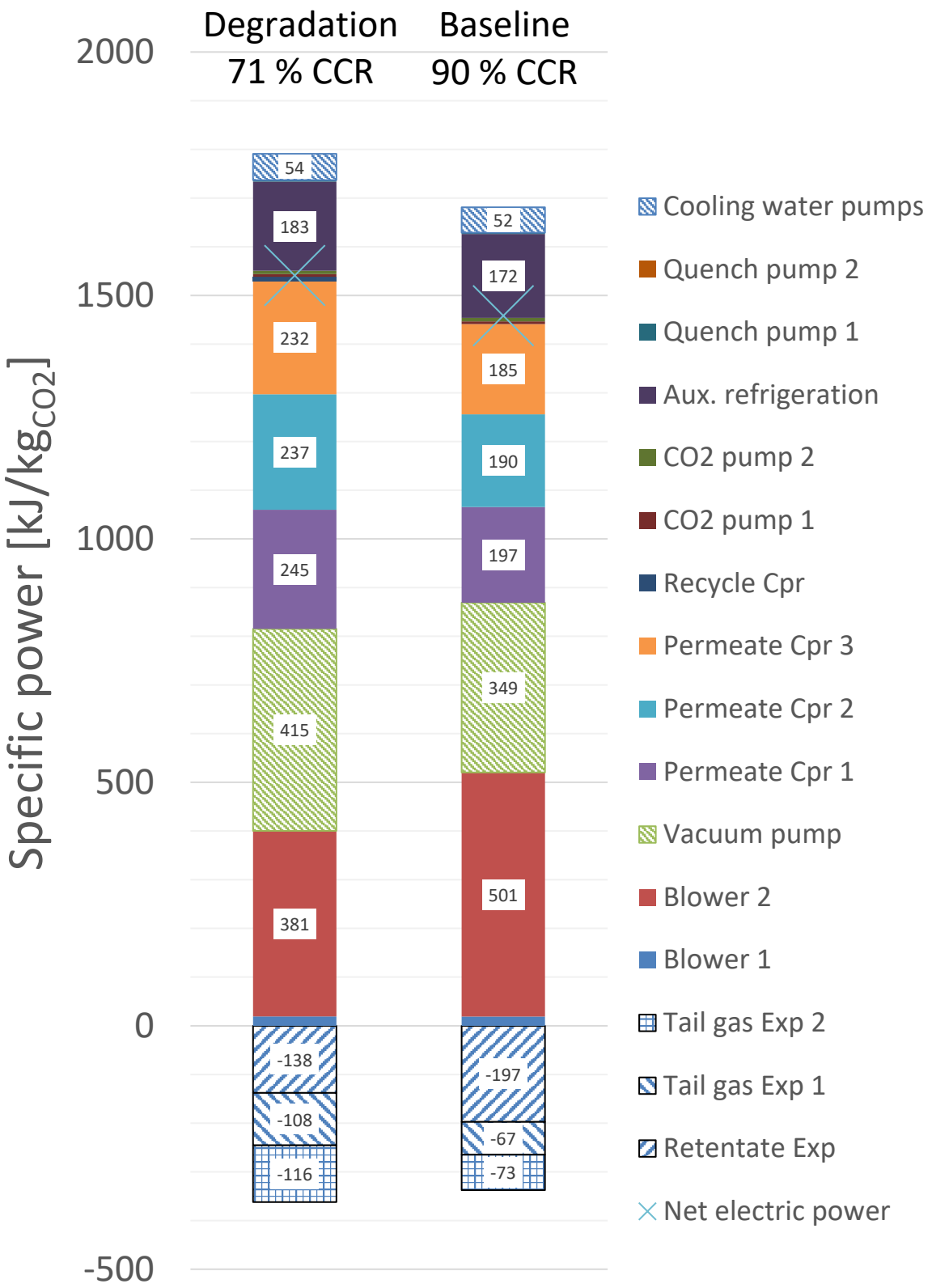

Figure 15. Decomposed specific power input and output results for Case no. 6.

This project has received funding from the European Union's Horizon2020 Research and Innovation Programme under Grant Agreement No 641185

6 SUMMARY OF RESULTS AND DISCUSSION

A summary of overall results for the different cases are given in Table 3.

Comparing results for "full capture" (90 % CCR) and partial capture (60 %) illustrates the issues of trying to achieve "full capture" by using membranes with characteristics as those given in this work (Table 2). Results show that without increasing the total membrane surface area beyond the already high area assumed, it is challenging to achieve simultaneously very high CO_2 capture ratio and at the same time favourable interfacial CO_2 concentration in the permeate gas, which makes the feed gas for the low-temperature CO_2 liquefaction unit. A favourable interfacial CO_2 concentration between the membrane bulk separation process and the low-temperature CO_2 liquefaction and purification process is typically well above 60 mol%. This specific electric power requirement for 90 % CO_2 capture ratio (1458 kJ/kg$_{CO2}$) is considerably higher than that for 60 % CO_2 capture ratio (1246 kJ/kg$_{CO2}$). A direct comparison of specific electric power requirement is shown in Figure 16.

Table 3. Summary of results

Case no.		**1**	**2**	**3**	**4**	**5**	**6**
Description		**Typical air leak, 90 % CO_2 capture**	**Low air leak, 90 % CO_2 capture**	**Typical air leak, 60 % CO_2 capture**	**Low air leak, 60 % CO_2 capture**	**Low air leak, 71 % CO_2 capture**	**Typical air leak, reduced CO_2/N_2 selectivity**
CO_2 concentration at membrane inlet[a]	mol%	20.17	24.17	18.91	23.48	23.71	20.59
CO_2 concentration at coldbox inlet	mol%	60.31	64.32	71.06	76.40	75.13	53.31
CO_2 capture ratio	%	90.0	90.2	59.9	60.5	70.9	76.0
Membrane area	m^2	228 000	228 000	152 000	152 000	152 000	228 000
Specific power	kJ/kg$_{CO2}$	1458	1253	1246	1066	1098	1541

[a] Membrane feed stream is aggregate of flue gas stream and recycle stream from CO_2 liquefier

There are several causes of the increase in specific power requirement between partial (60 %) and full capture (90 %). 90 % capture requires generally higher degree of flue gas pressurisation (2.55 bar(a) for 90 % capture vs. 1.6 bar(a) for 60 % capture) to increase the permeation of CO_2, the concentration of which is decreasing through the membrane from the inlet to the retentate outlet. The increased requirement for flue gas compression increases the overall power requirement substantially, as very large volumes of gas need to be compressed.

This project has received funding from the European Union's Horizon2020 Research and Innovation Programme under Grant Agreement No 641185

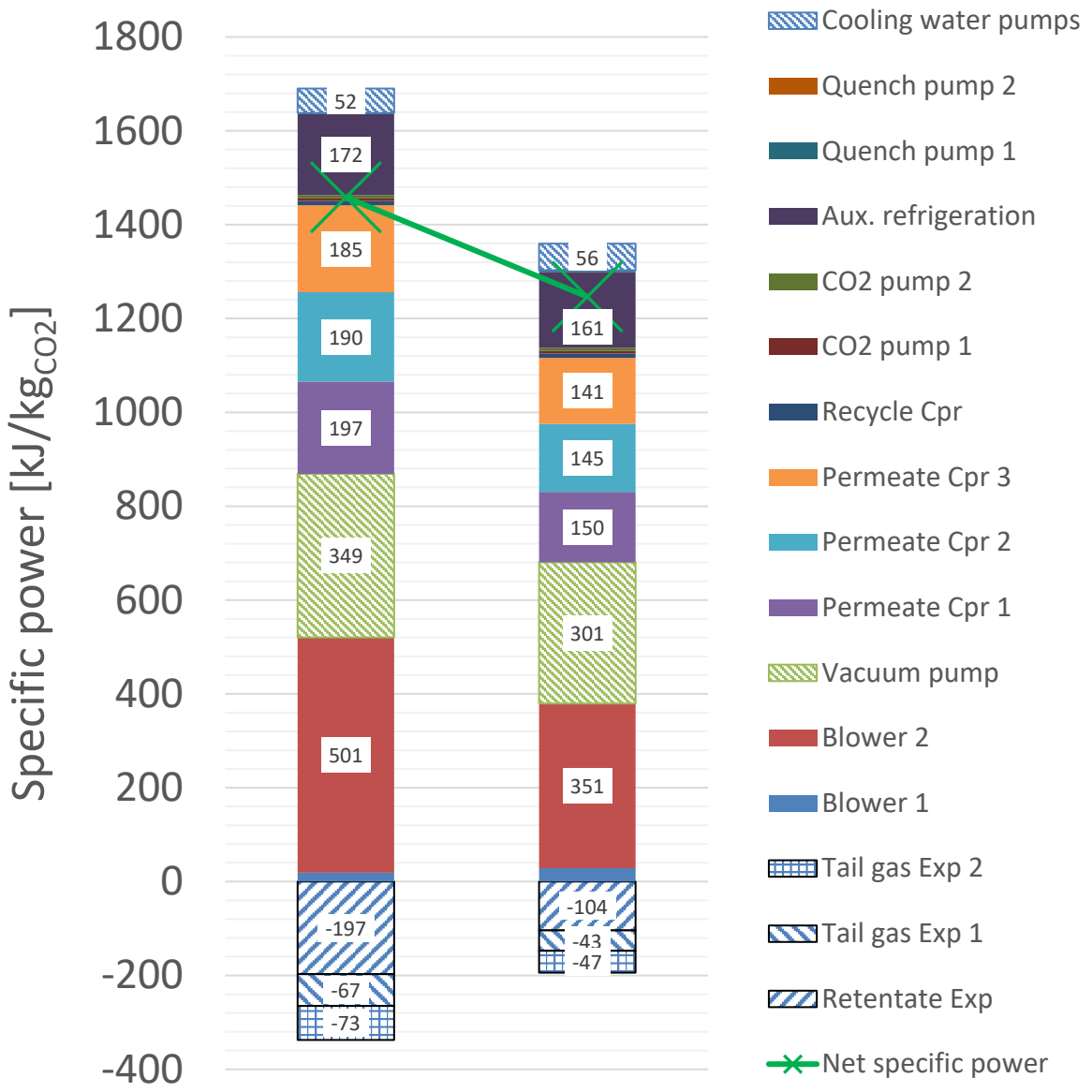

Figure 16. Comparison of specific electric power requirement between 90 % (left) and 60 % (right) CO_2 capture ratio. Both cases assume typical-air-leak flue gas feed conditions.

Through higher pressure difference between the feed and permeate side, the flux of nitrogen and other undesirable diluents also increase, which in turn limits the achieved CO_2 concentration in the permeate gas. Whereas the permeate gas after drying has 71 mol % CO_2 concentration in the typical air leak 60 % case, the corresponding number for the 90 % case is only 60.3 mol%. This has implications on the specific power requirement in the low-temperature CO_2 liquefaction unit. The compression of more diluted CO_2 increases the specific power requirement for permeate compression, both from vacuum pressure (0.2 bar(a)) to atmospheric pressure, and thereafter from atmospheric pressure to high pressure (about 32 bar before aftercooling) in the permeate compressor train.

An additional negative effect of lower CO_2 concentration in the permeate is the reduced CO_2 liquid yield in the CO_2 liquefaction process, for which the internal liquid-CO_2 yield equals about 78 %

This project has received funding from the European Union's Horizon2020 Research and Innovation Programme under Grant Agreement No 641185

versus 87 % for 60 % capture. This leads in turn to higher degree of gas recirculation from the first separator back to the membrane feed, which in overall adds to the net power requirement, as well as to the required membrane surface area.

In addition to targeted CO_2 capture ratio, the performance of the membrane-assisted CO_2 liquefaction capture process is sensitive also to the flue gas CO_2 concentration. As can be observed from the overall results in Table 3, the specific power requirement is significantly reduced when flue gas characteristics change from typical air leak (18 mol% CO_2) to low air leak (22 mol% CO_2). From the simulation results, specific power requirement is reduced by about 14 % for both the 90 % capture case and the 60 % CO_2 capture case. Figure 17 compares power results for 90 % capture for typical air leak and low air leak flue gas conditions.

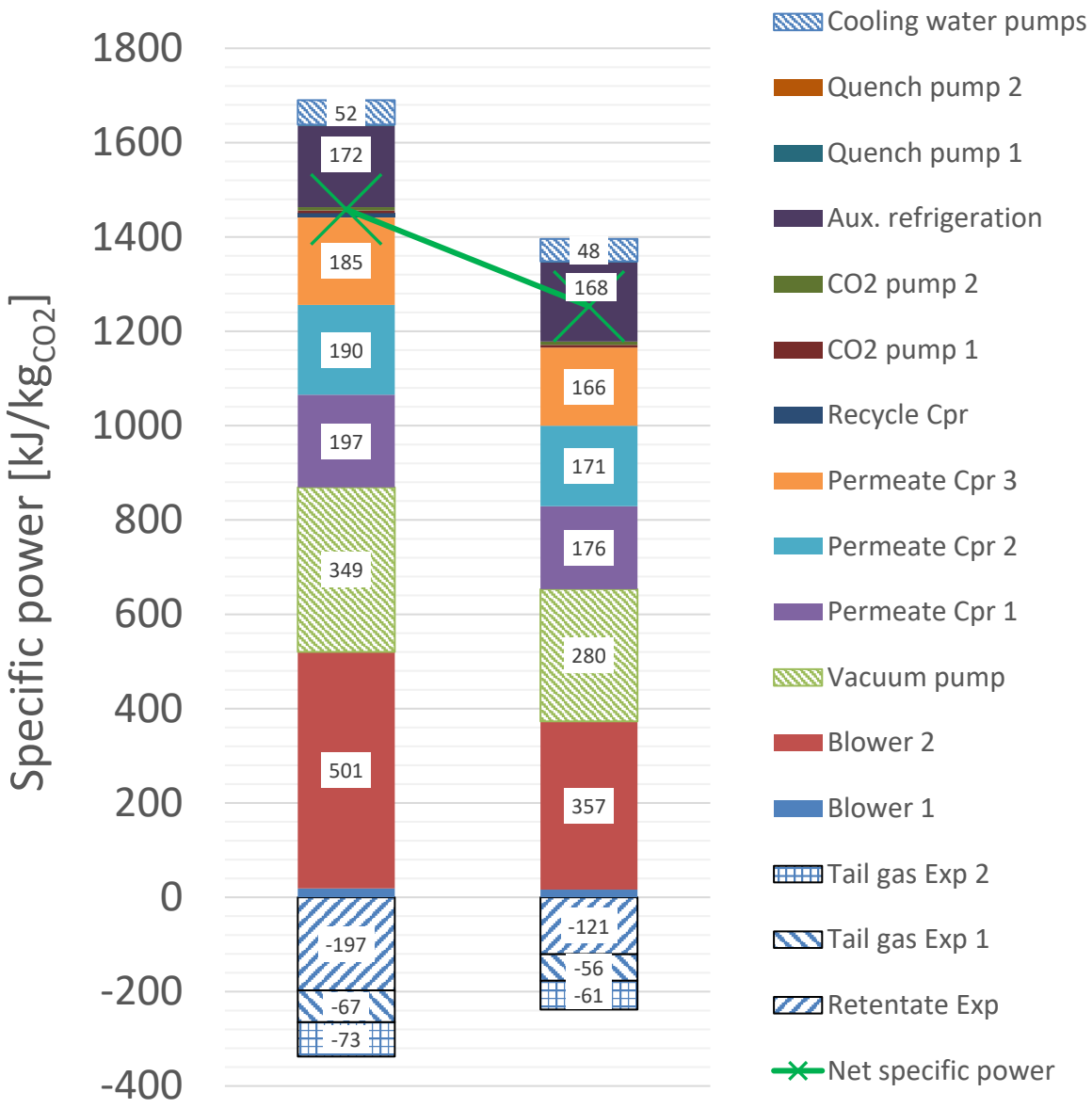

Figure 17. 90 % CO_2 capture ratio: Comparison of specific electric power requirement between typical air leak (left) and low air leak (right) flue gas conditions.

This project has received funding from the European Union's Horizon2020 Research and Innovation Programme under Grant Agreement No 641185

There are several contributing factors to the reduction of specific power requirement for low air leak versus typical air leak. Reduced flue gas pressurisation for the low air leak case (2.28 bar(a) vs. 2.55 bar(a)) lowers the power requirement of the main blower ("Blower 2"). A slightly increased vacuum-side pressure (0.23 bar(a) vs. 0.20 bar(a)) reduces the vacuum pump power demand. The permeate CO_2 concentration after dehydration is 64.3 mol% for the low air leak case, which results in lower permeate compressor power as well as higher liquid CO_2 yield in the liquefaction process. These effects contribute altogether to about 14 % lower specific power requirement.

For the 60 % CO_2 capture cases, the same qualitative descriptions apply for explaining the 14 % reduction in specific power requirement for low air leak relative to that for typical air leak.

This project has received funding from the European Union's Horizon2020 Research and Innovation Programme under Grant Agreement No 641185

7 CONCLUSIONS AND FURTHER WORK

Six different cases have been simulated on a process level for CO_2 capture from flue gas from a cement plant, using a hybrid gas separation process. The first separation stage uses a polymeric membrane for bulk separation of CO_2 from the flue gas, from which the vacuum-side permeate becomes a crude CO_2 stream requiring further purification to adhere to transport and storage purity specifications. The membrane has a CO_2 permeance of 2.7 $m^3(STP)m^{-2}bar^{-1}h^{-1}$, and a selectivity of 50 for CO_2 over nitrogen. In the second separation stage CO_2 is separated from the diluents by compression, refrigeration and phase separation. The CO_2-rich gaseous separation product is recycled to the membrane separation unit.

Two different flue gas compositions have been considered, with CO_2 concentration of 18 mol% ("Typical air leak") and 22 mol% ("Low air leak"), respectively. For each of the flue gas compositions, two different CO_2 capture ratios have been targeted: 90 % and 60 %. In the two remaining cases, no particular CO_2 capture ratios have been targeted, but rather been calculated as a function of changes in operational parameters while keeping the membrane surface area unaltered. The last of the simulated cases is a "what-if" case in which membrane degradation is assumed in the form of increased nitrogen permeance, reducing the CO_2 selectivity over nitrogen to 25.

The main result of interest in the present work is the aggregate energy requirement for the CO_2 capture processes. The membrane-assisted CO_2 liquefaction process has no high-temperature thermal energy requirements and therefore requires only power as energy input. The estimated specific electric power requirement varies between 1066 kJ/kg_{CO2} (low air leak, 60 % CO_2 capture ratio) and 1458 kJ/kg_{CO2} (typical air leak, 90 % CO_2 capture ratio). For the last case considered, in which the membrane's CO_2 selectivity is reduced to 25, the net electric power requirement is 1541 kJ/kg_{CO2} (typical air leak, 76 % CO_2 capture ratio). In all cases, the dominant drivers for power consumption are: blower power for flue gas compression, vacuum pumping of crude CO_2 permeate, compression of crude CO_2 permeate and auxiliary refrigeration.

Performance of the membrane-based separation process is highly sensitive to the flue gas CO_2 concentration. The specific power requirement at low air leak (22 mol% CO_2) is significantly lower than at typical air leak (18 mol% CO_2), by a margin of 14 %. For end-of-pipe CO_2 capture from cement kilns with less air infiltration and thus higher CO_2 concentration than assumed in the present study, the general performance of the membrane-assisted CO_2 liquefaction process will improve substantially. A favourable interfacial CO_2 concentration between the membrane bulk separation process and the low-temperature CO_2 liquefaction and purification process is typically well above 60 mol% (dry basis) and is significantly easier to obtain with increasing flue gas CO_2 concentration.

The membrane with characteristics as assumed in this work seems, particularly from the viewpoint of energy requirement, and given the current flue gas characteristics, to be better suited for partial capture (e.g. 60 %) than for full capture (e.g. 90 %). This view can likely be generalised to apply for the principle of membrane-based, end-of-pipe post-combustion CO_2 technology, due to the inherent trade-off and compromise between removing a high portion of CO_2 and at the same time retaining high permeate CO_2 purity. For higher flue gas CO_2 concentrations, beyond those considered in this work, however, the performance of membrane separation as well as membrane-assisted CO_2 liquefaction will increase considerably, so this conclusion will change depending on the actual flue gas CO_2 concentration in consideration.

This project has received funding from the European Union's Horizon2020 Research and Innovation Programme under Grant Agreement No 641185

Further work on membrane-assisted CO_2 liquefaction should focus on identifying suitable membranes in terms of permeabilities and selectivity. There is recent work in the literature [6] that investigates this methodically for membrane-based post-combustion CO_2 capture processes. However, it is expected that "optimal" membrane properties required for hybrid membrane-assisted liquefaction processes will be different than those considered optimal for capture processes entirely based on membrane separation in multiple stages. Compared to other capture technologies, the performance of membrane-based solutions is highly susceptible to CO_2 concentrations in the flue gas stream. Thus, it is important to look at opportunities for reducing air ingress and thus increasing CO_2 concentrations, as this can considerably improve the performance of membrane-assisted CO_2 liquefaction relative to other solvent- and sorbent-based post-combustion capture technologies.

This project has received funding from the European Union's Horizon2020 Research and Innovation Programme under Grant Agreement No 641185

ACKNOWLEDGEMENTS

This project has received funding from the *European Union's Horizon 2020 research and innovation programme* under grant agreement No 641185.

REFERENCES

[1] CEMCAP deliverable D3.2 – CEMCAP framework for comparative techno-economic analysis of CO_2 capture from cement plants
[2] CEMCAP deliverable D4.3 – First CEMCAP cement plant processes with CO_2 capture
[3] S. Roussanaly, R. Anantharaman, K. Lindqvist, H. Zhai, E. Rubin. Membrane properties required for post-combustion CO_2 capture at coal-fired power plants, Journal of Membrane Science 511, 2016, p. 250–264.
[4] A. Wexler. Journal of Research of the National Bureau of Standards, 81A, 1977, p. 5–20.
[5] E.W. Lemmon et al. NIST Standard Reference Database 23, version 9.0
[6] S. Roussanaly, R. Anantharaman, K. Lindqvist, B. Hagen. A New Approach to the Identification of High-Potential Materials for Cost-Efficient Membrane-Based Post-Combustion CO_2 Capture." Sustainable Energy Fuels, 2, 2018, p. 1225–1243. https://doi.org/10.1039/C8SE00039E

This project has received funding from the European Union's Horizon2020 Research and Innovation Programme under Grant Agreement No 641185

APPENDIX

A APPENDIX – SIMULATION DATA FOR TYPICAL AIR LEAK, 90 % CO_2 CAPTURE

	Power	Specific power
	kW	kJ/kg_{CO2}
Blower 1	479	19
Blower 2 (Main)	12678	501
Vacuum pump	8815	349
Permeate compressor 1	4968	197
Permeate compressor 2	4813	190
Permeate compressor 3	4687	185
Recycle compressor	233	9
CO_2 pump 1	140	6
CO_2 pump 2	178	7
Auxiliary refrigeration	4388	174
Quench pump 1	68.3	3
Quench pump 2	0.3	0
Cooling water pumps	1348	53
Retentate Expander	-5179	-205
Tail gas Expander 1	-1705	-67
Tail gas Expander 2	-1838	-73
Net electric power requirement	36763	1454
CO_2 capture rate [kg/h]	91019.6	

This project has received funding from the European Union's Horizon2020 Research and Innovation Programme under Grant Agreement No 641185

B APPENDIX – ENERGY RESULTS FOR LOW AIR LEAK, 90 % CO_2 CAPTURE

	Power	Specific power
	kW	kJ/kg_{CO2}
Blower 1	409	16
Blower 2 (Main)	8971	357
Vacuum pump	7069	282
Permeate compressor 1	4448	177
Permeate compressor 2	4307	172
Permeate compressor 3	4188	167
Recycle compressor	231	9
CO_2 pump 1	140	6
CO_2 pump 2	176	7
Auxiliary refrigeration	4228	168
Quench pump 1	59	2
Quench pump 2	0.27	0
Cooling water pumps	1226	49
Retentate Expander	-3360	-134
Tail gas Expander 1	-1431	-57
Tail gas Expander 2	-1544	-61
Net electric power requirement	31301	1247
CO_2 capture rate [kg/h]	90375.0	

This project has received funding from the European Union's Horizon2020 Research and Innovation Programme under Grant Agreement No 641185

C APPENDIX – ENERGY RESULTS FOR TYPICAL AIR LEAK, 60 % CO_2 CAPTURE

	Power	Specific power
	kW	kJ/kg_{CO2}
Blower 1	479	28
Blower 2 (Main)	5916	351
Vacuum pump	5068	301
Permeate compressor 1	2526	150
Permeate compressor 2	2443	145
Permeate compressor 3	2368	141
Recycle compressor	155	9
CO_2 pump 1	94	6
CO_2 pump 2	118	7
Auxiliary refrigeration	2713	161
Quench pump 1	66.6	4
Quench pump 2	0.8	0
Cooling water pumps	949.4	56
Retentate Expander	-1752	-104
Tail gas Expander 1	-729	-43
Tail gas Expander 2	-790	-47
Net electric power requirement	20993	1246
CO_2 capture rate [kg/h]	60633.2	

This project has received funding from the European Union's Horizon2020 Research and Innovation Programme under Grant Agreement No 641185

D APPENDIX – ENERGY RESULTS FOR LOW AIR LEAK, 60 % CO_2 CAPTURE, OFF-DESIGN CASE

	Power	Specific power
	kW	kJ/kg_{CO2}
Blower 1	409	24
Blower 2 (Main)	2825	168
Vacuum pump	4612	274
Permeate compressor 1	2266	134
Permeate compressor 2	2189	130
Permeate compressor 3	2116	126
Recycle compressor	155	9
CO_2 pump 1	94	6
CO_2 pump 2	118	7
Auxiliary refrigeration	2641	157
Quench pump 1	57.6	3
Quench pump 2	0.8	0
Cooling water pumps	869	52
Retentate Expander	-254	-15
Tail gas Expander 1	-557	-33
Tail gas Expander 2	-605	-36
Net electric power requirement	17973	1066
CO_2 capture rate [kg/h]	60699.0	

This project has received funding from the European Union's Horizon2020 Research and Innovation Programme under Grant Agreement No 641185

E APPENDIX – ENERGY RESULTS FOR LOW AIR LEAK, 71 % CO_2 CAPTURE, OFF-DESIGN CASE

	Power	Specific power
	kW	kJ/kg_{CO2}
Blower 1	409	21
Blower 2 (Main)	4838	245
Vacuum pump	5298	268
Permeate compressor 1	2717	138
Permeate compressor 2	2626	133
Permeate compressor 3	2540	129
Recycle compressor	182	9
CO_2 pump 1	110	6
CO_2 pump 2	138	7
Auxiliary refrigeration	3113	158
Quench pump 1	58.1	3
Quench pump 2	0.7	0
Cooling water pumps	971	49
Retentate Expander	-1267	-64
Tail gas Expander 1	-671	-34
Tail gas Expander 2	-727	-37
Net electric power requirement	21678	1098
CO_2 capture rate [kg/h]	71093.9	

This project has received funding from the European Union's Horizon2020 Research and Innovation Programme under Grant Agreement No 641185

F APPENDIX – ENERGY RESULTS TYPICAL AIR LEAK BASE CASE WITH REDUCED CO_2 SELECTIVITY

	Power	Specific power
	kW	kJ/kg_{CO2}
Blower 1	414	19
Blower 2 (Main)	8140	381
Vacuum pump	8863	415
Permeate compressor 1	5229	245
Permeate compressor 2	5070	237
Permeate compressor 3	4954	232
Recycle compressor	196	9
CO_2 pump 1	119	6
CO_2 pump 2	151	7
Auxiliary refrigeration	3910	183
Quench pump 1	67.2149991	3
Quench pump 2	4.52E-02	0
Cooling water pumps	1150	54
Retentate Expander	-2946	-138
Tail gas Expander 1	-2303	-108
Tail gas Expander 2	-2487	-116
Net electric power requirement	32928	1541
CO_2 capture rate [kg/h]	76919.4	

This project has received funding from the European Union's Horizon2020 Research and Innovation Programme under Grant Agreement No 641185